SIZE SEGREGATION OF BINARY GRANULAR MATERIALS IN VERTICAL CHANNEL FLOWS

Thesis by

Susan M. Beatty

In Partial Fulfillment of the Requirements
for the Degree of
Mechanical Engineer

Division of Engineering and Applied Science
California Institute of Technology
Pasadena, California

1993
(Submitted October 2, 1992)

ACKNOWLEDGEMENTS

I wish to thank my advisors, professors M. Hunt, C. Brennen, and A. Acosta for their advice and support. Thanks to Marty Gould for his ideas and help. A special thanks to my husband and children for their sacrifice, support and encouragement.

This thesis is dedicated to my father, who gave me his love of engineering and science, and quest for knowledge and higher education, without whose encouragement I probably would never have attempted this endeavor.

ABSTRACT

This experimental research investigates transverse particle segregation in a binary mixture of spherical particles in air, in a gravity driven, vertical channel flow. Glass beads with similar properties, except for size and color, are randomly mixed in an upper hopper at the entrance of a vertical channel. When roughened channel walls are employed, particles show segregation by size, with a preferred position of larger particles at the centerline and approximately 80% of the distance between the centerline and the side walls. The concentration of the particles is found based on grey-scale color distribution as recorded by an image processing system. The effects of variations in flow rate, wall surface conditions, mixture ratios and channel width on segregation are studied as a function of downstream distance.

TABLE OF CONTENTS

LIST OF TABLES

LIST OF FIGURES

I. INTRODUCTION - SEGREGATION OF GRANULAR MATERIALS

Granular materials may be composed of particles varying in size, density, shape and surface characteristics. Under motion, these materials tend to segregate, with particles of similar size coalescing. Particle segregation by size appears to exist even when differences in density or other physical characteristics are present (Williams 1976). Studies of segregation due to size have shown that percolation of smaller particles occurs when a mass of particles is disturbed in the presence of a gravitational field. Gaps occurring within the particle packing allow these particles to move downward through the material. This behavior has been studied for several flow geometries. These studies have not attempted to study segregation occurring in the direction transverse to a gravity field.

An early segregation study was performed by Donald and Roseman (1962), who investigated radial segregation in a rotating horizontal drum. Radial segregation was observed: the finer material concentrated in a central core parallel to the axis of rotation with the larger particles surrounding the core at the outer periphery. This type of segregation behavior may be explained by reference to the "heap pouring" effect: finer particles are sieved out from the highly sheared surface layer and accumulate in the comparatively static and undeformed central region. As rotation continued, axial segregation occurred, the effect starting at the end plates with alternating layers of the components showing a series of stripes running perpendicular to the axis. Differing angles of dynamic repose in the drum were determined to be the cause of the segregation

in the axial direction.

Several investigators have studied the effect of vibration on a mass of granular particles. Williams and Shields (1967) studied segregation occurring when a stream of particles containing a mix of two sizes was fed continuously over a vibrating plate while varying the direction of vibration. They found that the greatest amount of segregation occurred for a direction of vibration 30 degrees from the horizontal. Campbell and Bridgwater (1973) studied the effect of a shear field as a cause of segregation in a powder mass. A bed of particles was contained between vertical walls of float glass. The bed rested on a piston which was driven downward to induce movement of the bed. One end wall of the container was roughened with sandpaper. When tracer particles of 2 mm diameter were observed in a bed of 4 mm particles, vertical percolation was noted in a zone extending 7 particle diameters. The width of the shear zone was velocity dependent varying from 5 to 15 particle diameters.

Foo and Bridgwater (1983) conducted experiments showing that a single, 12 mm diameter, large particle in a bed of smaller, 6 mm diameter, particles, moved toward the region of greater mobility of the smaller particles, i.e., in the direction of increasing strain rate. This motion was caused by a greater frequency of void occurrence in one direction due to a higher strain rate. Where small particles on one side of a larger sphere are stationary, the large particle can only move away from the stationary particles toward the mobile ones.

Savage and Lun (1988) proposed two main mechanisms responsible for size segregation in two-dimensional flows containing binary mixtures of large and small

spherical particles. The flow was assumed to take place in layers that were in motion relative to each other due to shear. The first mechanism is gravity induced, referred to as the "random fluctuating sieve"; the second, the "squeeze expulsion mechanism" is due to an unbalance of contact forces on a particle which squeeze it out of its own layer into another. Net percolation of smaller particles downward is due to a combination of the two mechanisms. Analytical and experimental results were found for flow down an inclined chute with glass side walls and a roughened lower surface. Experimentally, a binary mixture of spherical polystyrene beads with a 0.59 diameter ratio was used. The larger particles were 1.6 mm in diameter; the depth of flow was from 10 to 15 mm. After the particles were allowed to travel down the chute, splitter plates were inserted into the flow allowing for collection of five vertical layers of the particles. The concentrations of the particles in each layer were then determined. Smaller particles were found to concentrate at the bottom of the chute.

To date, researchers have noted several possible mechanisms responsible for segregation. In flowing materials, however, interest has been focused on segregation in the vertical direction, in which gravity plays a large role. As holes open in the mass matrix, smaller particles have a tendency to "fall" into the holes and percolate downward. Predictions of segregation based on differences in shearing of adjacent layers of particles have also been made, but in most cases the combination of gravitational and shear rate differences accounts for the percolation of particles. This past work suggests the need to measure migration of particles in the direction transverse to the gravitational vector; for these flows, segregation would be primarily due to the shearing of the flow, rather than

gravitational percolation effects.

Since some similarities can be drawn between granular material flows and that of Newtonian fluids, the movement of solid particles in liquids may show some similarities to large particles moving within a mass of smaller particles. Segré and Silberberg (1962) noted the behavior of solid particles traveling in a poiseuille flow. Their work studied a suspension of spherical particles in a liquid with a density within 1% of the density of the spheres. This mixture travelled through a vertical tube while measurements were made of the radial position of the particles within the flow stream. It was found that a rigid sphere is subjected to radial forces which tend to carry it to an equilibrium position at about 60% of the tube radius from the axis, irrespective of the radial position at which the sphere first entered the tube. The results from this study are shown in figure 1. Distributions measured are independent of the overall concentration of particles.

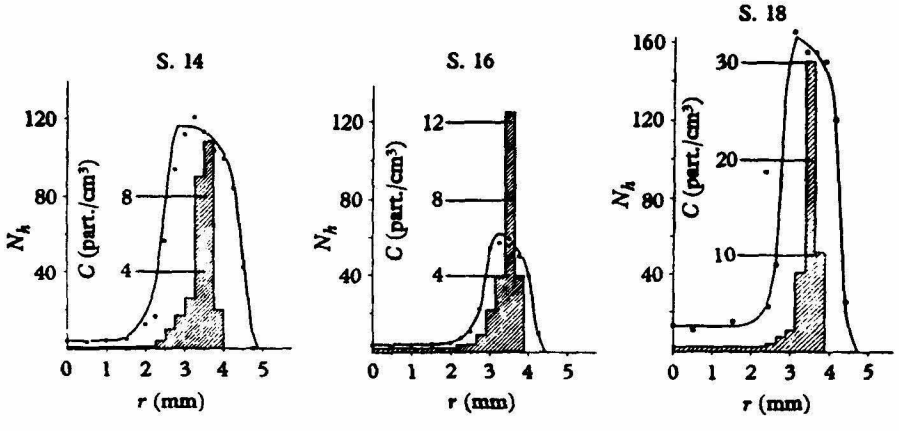

Figure 1. Results of Segré and Silberberg. Preferred position of neutrally buoyant particles in tubular Poiseuille flow. Particle concentration a maximum at 60% of tube radius from axis.

McTigue, Givler and Nunziato (1986) continued the work of Segré and Silberberg by studying planar poiseuille flow in a vertical channel. A nonuniform distribution of

particles across the channel is established as noted by Segré and Silberberg. McTigue, Givler and Nunziato also found that the concentration profile shape is a function of the buoyancy of the particles. If the particle is neutrally buoyant, the previous Segré, Silberberg results are confirmed, with peak concentrations occurring around 60% of the centerline to wall distance. The concentration profiles of the particles are dependent on the density of the particle relative to the liquid in which it is suspended, as well as the mean flow rate.

Transverse motion, leading to segregation of a mixture of two sizes of spherical glass particles moving through a vertical channel, is the focus of the current study. Since previous studies of suspensions have shown particles to have a preferred position within the channel, a similar trend can be sought for granular materials. This segregation is present in the direction transverse to the gravitational vector, therefore results of other segregation mechanisms without the influence of gravity may be measured.

II. EXPERIMENTAL PROGRAM

A. Introduction

Measurements of transverse concentration profiles within a vertical channel were made over a range of variables. A random mixture of dyed glass spheres with a diameter ratio of 0.5 was allowed to flow under gravity. The concentration of particles, based on the time averaged color at a given fixed location within the channel, is found using an image processing system.

B. Test Facility

The vertical channel employed in these experiments is shown in figure 3. The randomly mixed particles enter the test section through an upper feed hopper. The test section is 1 meter in height, 2.06 cm in depth. The front and back walls are made of glass. Two sets of side walls, that can be adjusted for variable channel width, are used: polished glass side walls and aluminum walls with 120° sawtooth grooves of 3 mm depth. The walls are spaced at either 3.81 cm or 5.08 cm apart for the experiments detailed.

Colored glass spheres of approximately equal density are used. Glass was selected to minimize the static attraction which may occur between particles when a material such as plastic is used. Blue, 4 mm diameter spheres, and yellow, 2 mm diameter spheres, were selected for this study. Previous researchers have obtained good results for particles

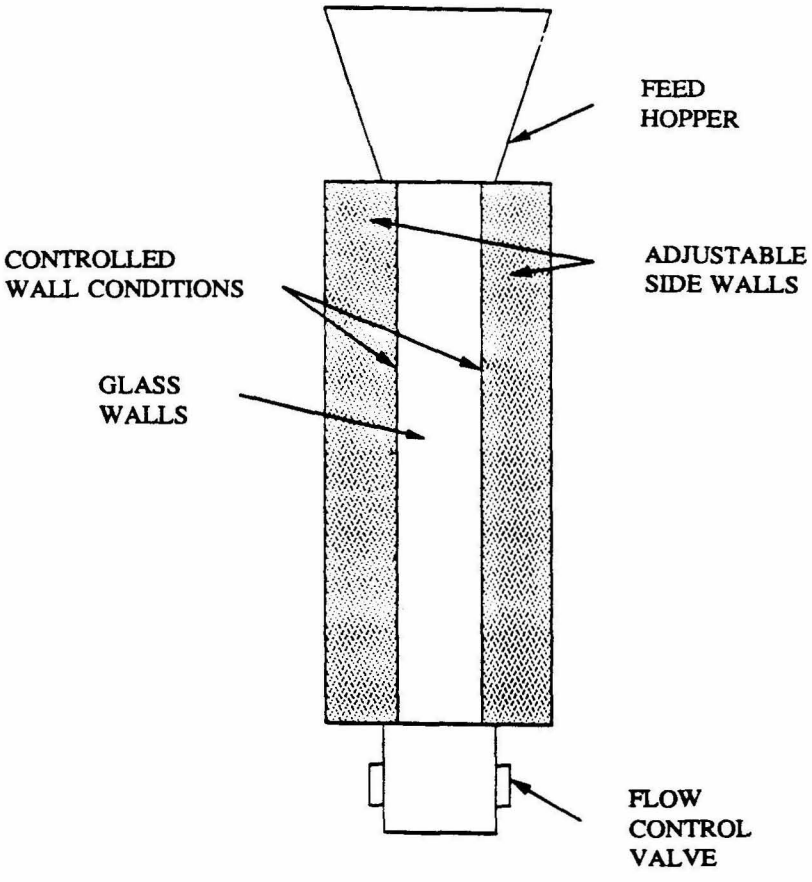

Figure 2. Experimental Facility

of similar size, and size ratio. The colors were selected to provide good contrast when filmed in black and white. Three weight ratios of particles were selected for study. As the segregation of particles is to be determined by the amount of each color as seen through the front glass of the test channel, ratios used were selected to provide a particle projected frontal area of 25% blue and 75% yellow; 50% blue and 50% yellow; or 25%

yellow and 75% blue. These ratios correspond to blue to yellow (large particle:small particle) mass ratios of 6:1, 2:1 and 2:3 respectively.

The rate of flow of the particles is controlled by the use of a valve at the exit of the test section. Three valve settings were used: the slowest flow setting was selected based on the minimum area the valve could be set to allow a free flow of particles, the fastest was based on that required to keep the channel filled with particles.

C. Image Recording

Data detailing changes in concentration consist of that obtained by image processing a series of frames recorded by a video camera. In order to obtain this data, a number of factors need be considered to obtain clear images.

This experimental facility employs a PC containing a video mux manufactured by EPIX, Inc. of Northbrook, Illinois. This card allows a PC to digitize, process, display, transmit and archive video information. It is used in conjunction with software produced by the same company, known as SVIP, which allows the user to digitize or display a sequence of images. Images may be read or written from/to a disk in TIFF (tagged image file format) and numerous routines including filtering, image enhancing and averaging over a series of frames are supported.

An image is obtained via a commercial super VHS video camera-recorder/player, (GR-270U manufactured by JVC) and is collected by the frame grabber. The image is divided into pixels with a maximum field width of 752 pixels and 240 pixel rows. Each

pixel has a grey scale value of 0 to 255, with 0 being black and 255, white.

Grey scale values are very sensitive to lighting, as well as color. For the purposes of this study, a high grey scale contrast between the two colors of particles used is imperative to allow differentiation of the particles sizes. It is also desirable to obtain consistent grey scale values for the same color of particle at various locations within the test channel. A number of variables in both camera recording and video capture of the flow exist that bear consideration.

Lighting of the channel must be uniform to observe segregation changes. Fluorescent tubes were attached to the front of the channel on either side of, and adjacent to, the side walls. This lighting arrangement provided a fairly uniform coverage of light over the length and width of channel. Since fluorescent tubes were used to illuminate the channel, the fluorescent lighting option was selected for the white balance on the camera.

The first problem encountered, was the contrast of bright light on the channel compared with darker surroundings. The lights were shielded, so that the image the camera observed, when automatically compensating to balance the light, was washed out. To correct for this, the shields over the fluorescent lights were covered with a glossy white contact paper and lights with reflectors were used to indirectly light the paper from the top and bottom of the channel. These additional lights reduced the contrast between the areas picked up by the white balance sensor window on the camera and produced clearer channel images.

Since a moving flow was to be studied, camera shutter speed was an important consideration. A rather interesting phenomenon occurred while trying to select an

optimum camera speed, that was believed to be due to automatic adjustments in the white balance.

The camera has a white balance sensor window which collects light and continually adjusts this balance. There is no way to manually override this setting. The amount of light entering the camera, along with the shutter speed selection, affects the grey scale pixel values obtained by the frame grabber. A study was undertaken to find the optimum setting required to produce a clear image of the flowing particles, as well as distinct pixel values produced by the two particle colors that had been selected.

The channel was filled with a mixture of the two particles. An area 1.14 cm long and 4.44 cm wide was observed. This area corresponds to 40 rows of pixels, with 120 pixels per row. With the particles remaining stationary, the camera speed was adjusted while all other variables remained constant to note the effect. There are four possible shutter speed selections: 1/60, 1/250, 1/500 and 1/1000 second. For each speed setting, data was obtained using the frame grabber. The period setting in the frame grabber program was 1/10 second for all cases. A total of 218 buffers of data were taken. (This is the maximum obtainable for a 40 x 120 pixel field)

Dramatic fluctuations of light recorded by the camera were present, particularly at higher shutter speeds. While looking through the camera, even with no recording taking place, the light intensity changed. Since this occurred while all manually adjustable camera settings are not changed, it is believed that white balance adjustment internal to the camera is changing the amount of light being allowed in the camera.

The data obtained with varying speed settings only is shown in figures 3 - 6.

Figure 3 shows a camera speed setting of 1/60 second; figure 4, 1/250 second; figure 5 1/500 second; figure 6, 1/1000 second. These curves show pixel values at a single random pixel location within the field over time. The curves shown are not at the same pixel location in each case, therefore the absolute magnitude of the pixel value is unimportant, but, the variation of pixel value is. The data are shown in their original, unfiltered condition. For most calculations the data were low-pass filtered before further use. Note that for a slow shutter speed of 1/60 second, data is fairly consistent over time (buffer). As the shutter speed is increased, the variation becomes more pronounced and definite cyclic behavior is noted.

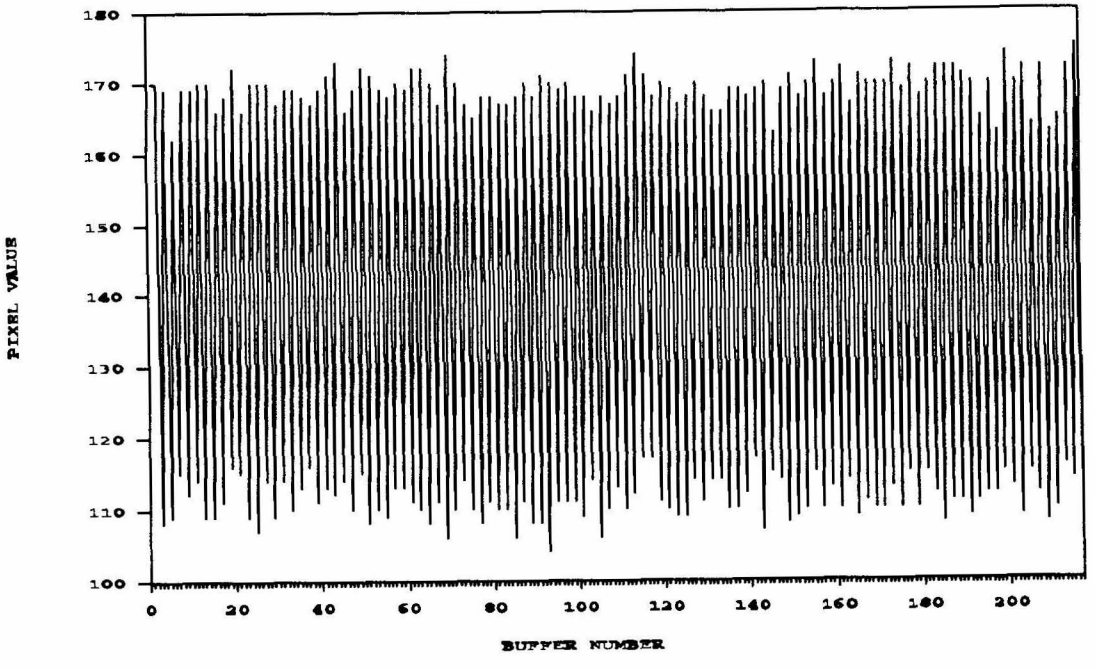

Figure 3. Pixel Value Data of Single Random Pixel
Camera Speed: 1/60 second

These curves reflect pixel value data at a single pixel location within the field. Conditions over the entire 40 x 120 pixel field are also of interest. To find how this pixel value variation affects the larger field, for each of the shutter speeds, 2 buffers were

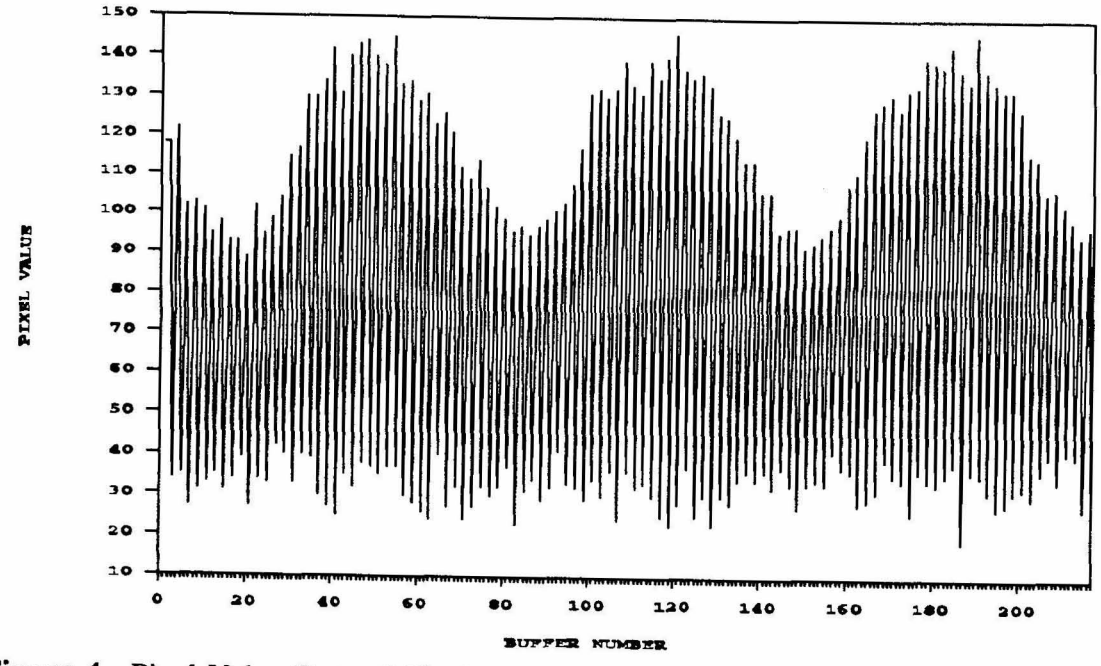

Figure 4. Pixel Value Data of Single Random Pixel
Camera Speed: 1/250 Second

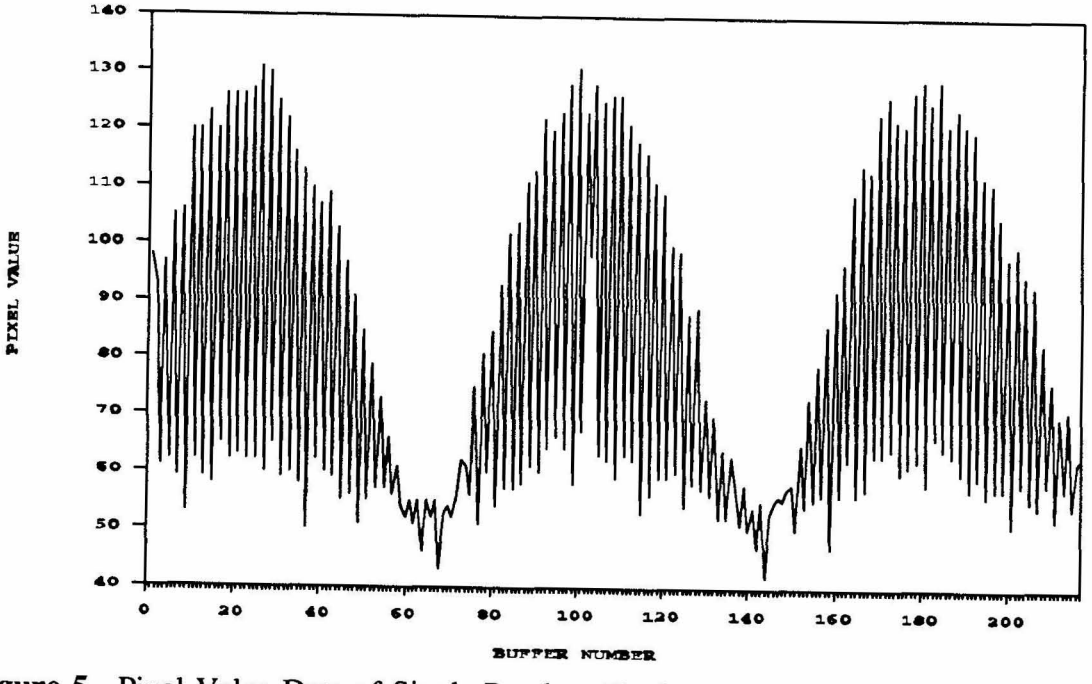

Figure 5. Pixel Value Data of Single Random Pixel
Camera Speed: 1/500 second

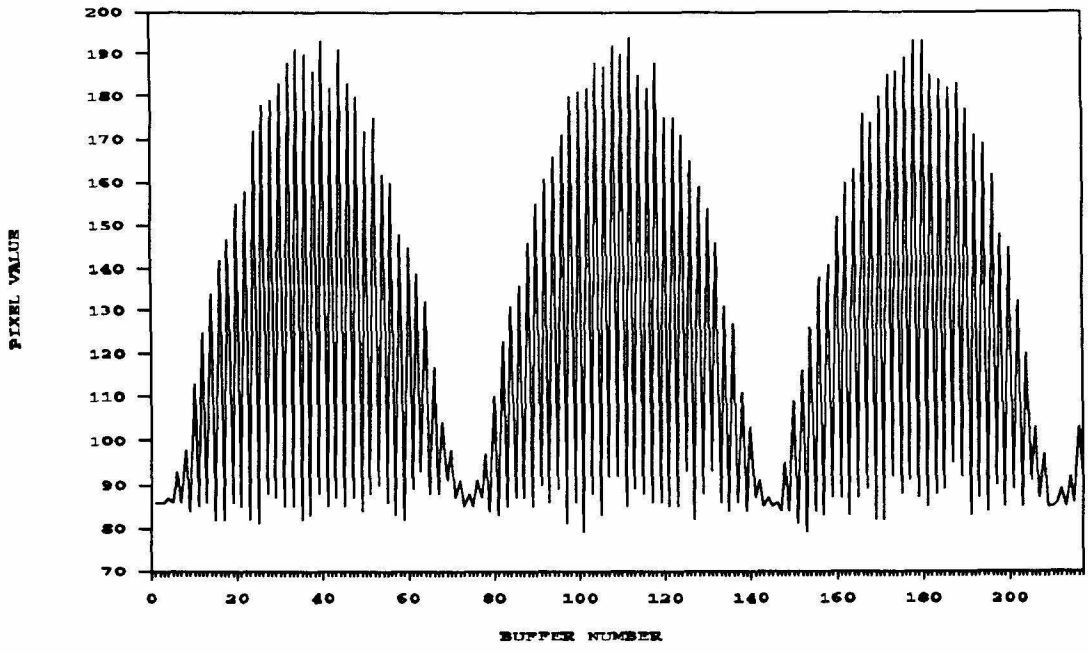

Figure 6. Pixel Value Data of Single Random Pixel
Camera Speed: 1/1000 second

selected, one at a maximum, one at a minimum based on the cyclic variations from the previous data set (figures 3 - 6). This data was low-pass filtered to remove variations other than the light changes. The histograms showing number of pixels for each pixel value over the grey scale range are shown in figures 7 -10. For this series of histograms, the fields used are identical, the same particles are being recorded in each case. The only manually selected variation is camera speed.

The 1/60 second case (figure 7) shows the pixel value data to be very consistent over the buffers as would be expected from the earlier data (figure 3). The blue particles exhibit a peak pixel value incidence of approximately 70, the yellow, 145. The 1/250 second case (figure 8) displays a shift between maximum and minimum lighting conditions on the order of 10 pixels. The average blue peak is about 75, yellow, 160. The 1/500 and 1/1000 cases confirm a large variation between the set of buffers. In

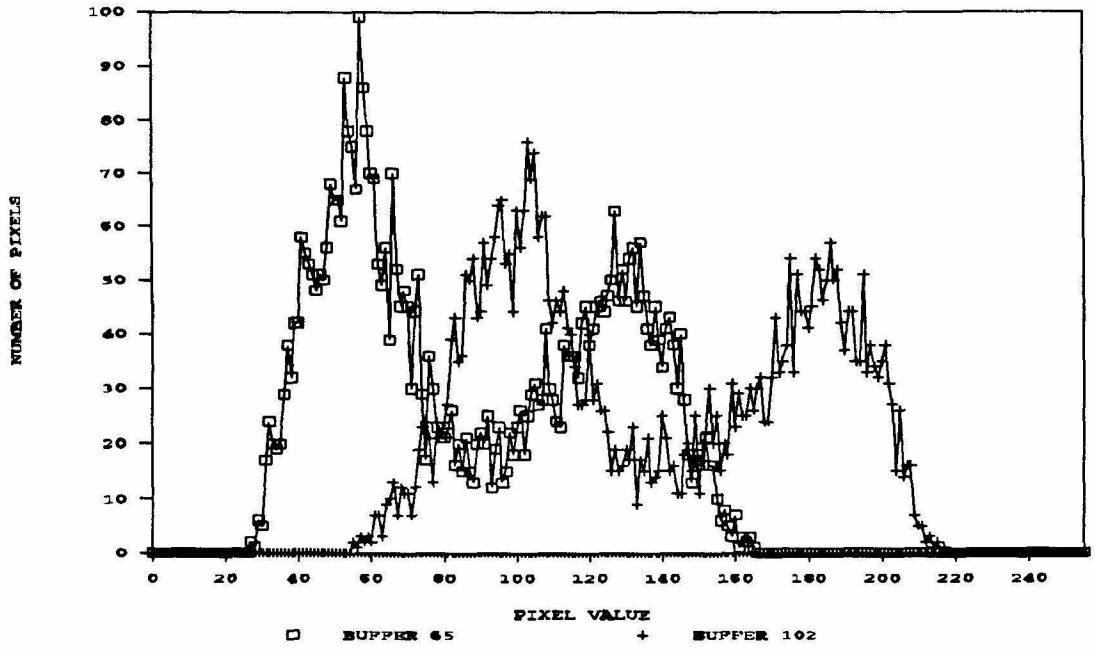

Figure 7. Histogram Data for 1/500 second Camera Speed

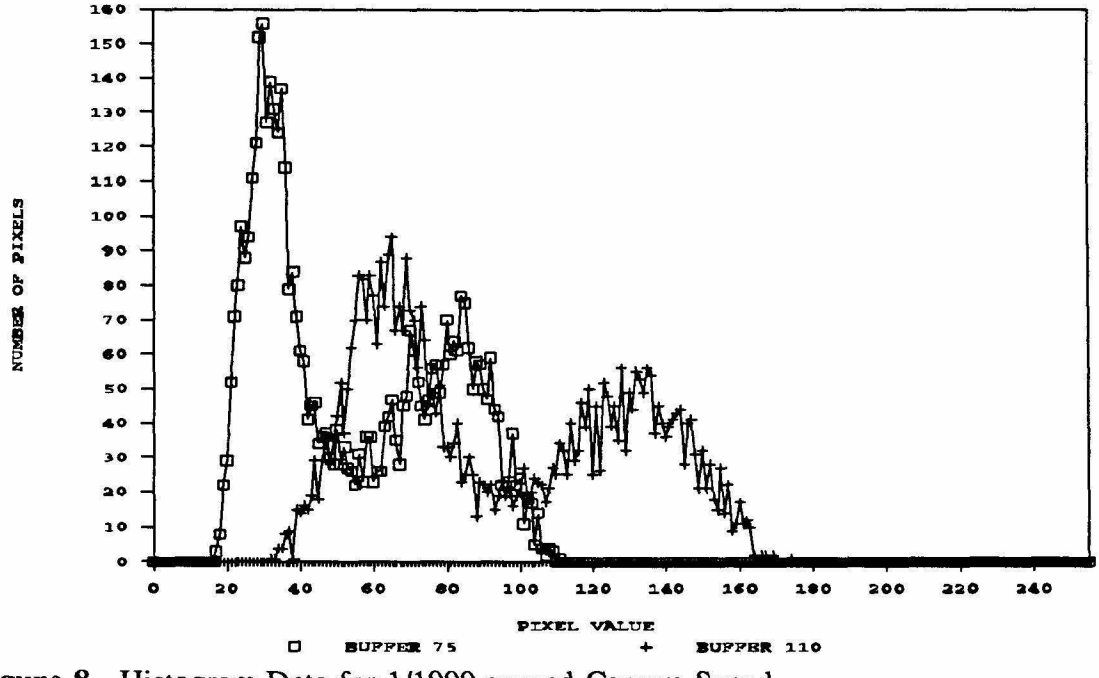

Figure 8. Histogram Data for 1/1000 second Camera Speed

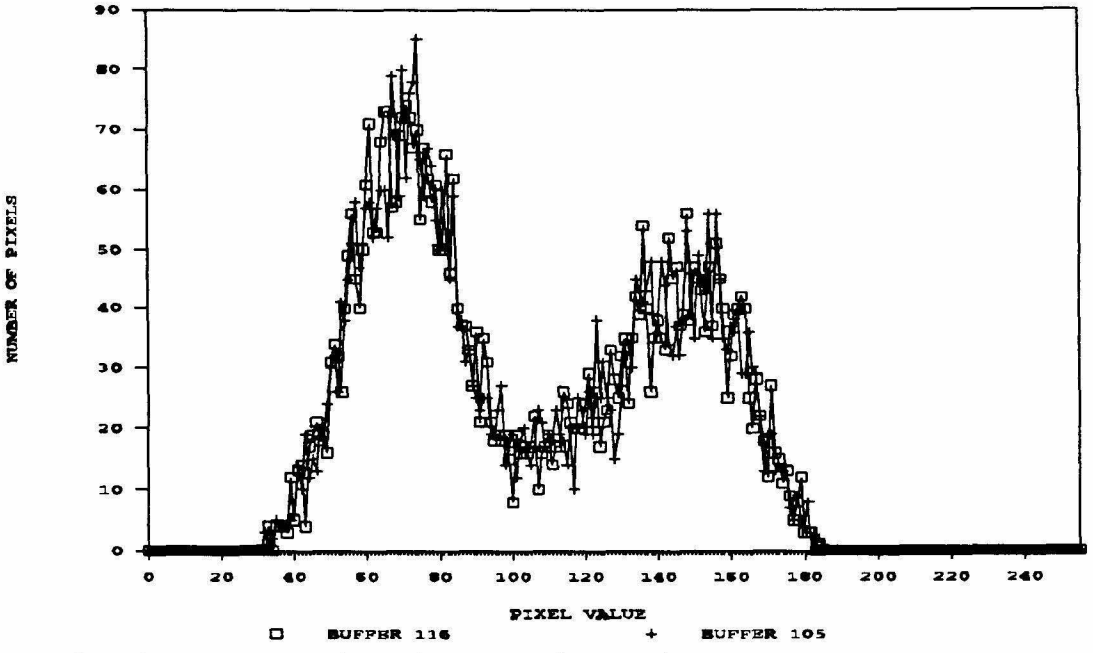

Figure 9. Histogram Data for 1/60 second Camera Speed

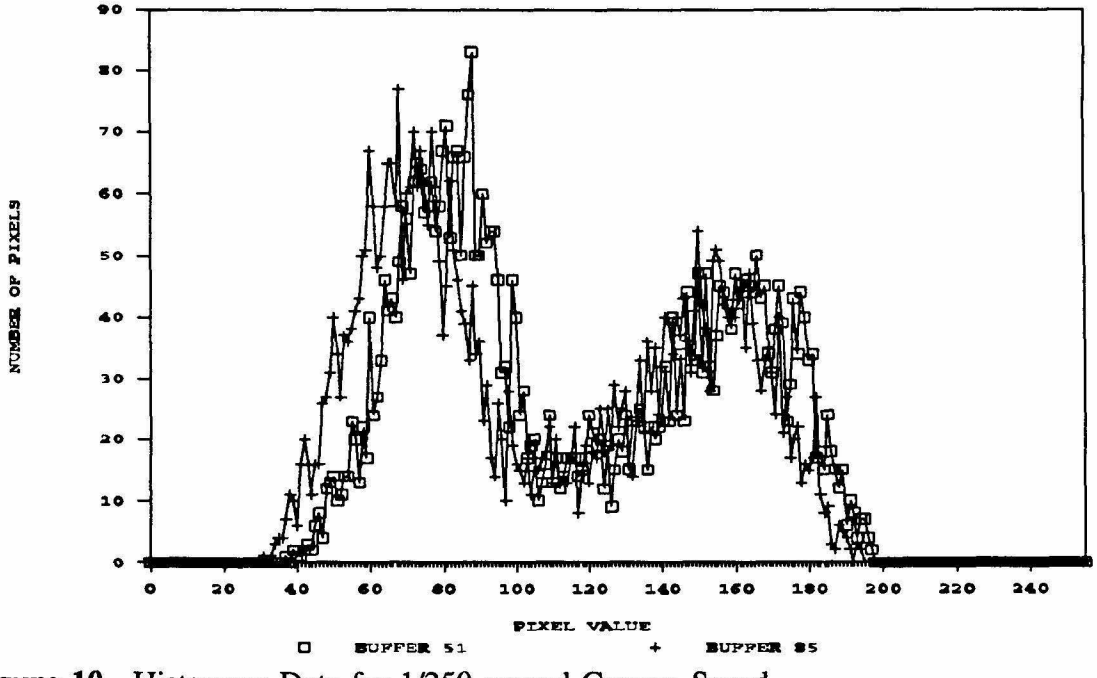

Figure 10. Histogram Data for 1/250 second Camera Speed

figure 9, the 1/500 second case indicates that under the minimum lighting conditions, peaks for blue and yellow were 55 and 130 respectively, and for the maximum lighting, 105 and 185, a shift of about 50 pixels. The 1/1000 second case also shows a 50 pixel value shift in the two peaks shown on the histogram for the same color.

Since such large shifts in pixel value readings for the identical set of particles, under constant external lighting, occur for the 1/500 and 1/1000 camera speeds, and because there is no way to over-ride the camera automatic light settings, these setting options were deemed unusable. The 1/60 case, which shows very consistent data, is not fast enough to capture crisp images when the flowing beads are filmed. Therefore, the 1/250 second setting was selected as the optimum camera shutter speed for the purpose. The shutter speed is fast enough so that crisp images may be obtained for flowing conditions if a proper selection of pixel size relative to particle size is made.

The pixel data were taken at four locations within the channel: channel entrance, 25 cm, 50 cm, and 75 cm from the channel entrance. The data were not taken near the channel exit since some flow distortion was present due to exit conditions.

The flow was filmed through the front glass wall of the channel, using a video camera, and stored on tape. Achievement of good resolution in the region being filmed necessitated moving the camera to focus on each of the four regions separately. Therefore, one test run was required for the filming of each location. A summary of test conditions for each run is shown in table 1.

In order to determine the extent of segregation in the vertical direction due to either segregation in the hopper before entrance to the channel, or, in the channel itself,

a sampling of particles at the channel discharge was taken. A mixture of particles with a large to small weight ratio of 2:3 and glass walls (test series 2 conditions) was allowed to flow through the channel. The particles were then collected in four approximately equal portions during the test run, the particle batches were sorted, weighed, and the mass

Table 1. Test Series Conditions *

Test Series	Wall Type	Mass Ratio Large:Small	Channel Width cm (2H)	Valve Setting cm
1	Glass	2:1	3.81	0.89
2	Glass	2:3	3.81	0.89
3	Sawtooth	2:1	3.81	0.89
4	Sawtooth	2:1	3.81	0.64
5	Sawtooth	2:1	3.81	1.14
6	Sawtooth	2:1	5.08	0.89
7	Sawtooth	2:3	3.81	0.89
8	Sawtooth	2:3	3.81	0.64
9	Sawtooth	2:3	3.81	1.14
10	Sawtooth	6:1	3.81	0.89

* Each test series includes measured data for each of 4 locations within the channel, repeated three times.

ratio determined for each of the four groups of particles. The mass ratio during the first half of the test remains constant, at the value originally input to the upper hopper. As the flow continues, segregation becomes apparent. The sampling taken during the third quarter of the run shows an increased flow of larger particles, resulting in a decrease in the amount of large particles available for the final quarter. Figure 11 presents the variation in mass ratio over the test.

This type of behavior has been documented by Arteaga and Tüzün (1990), who

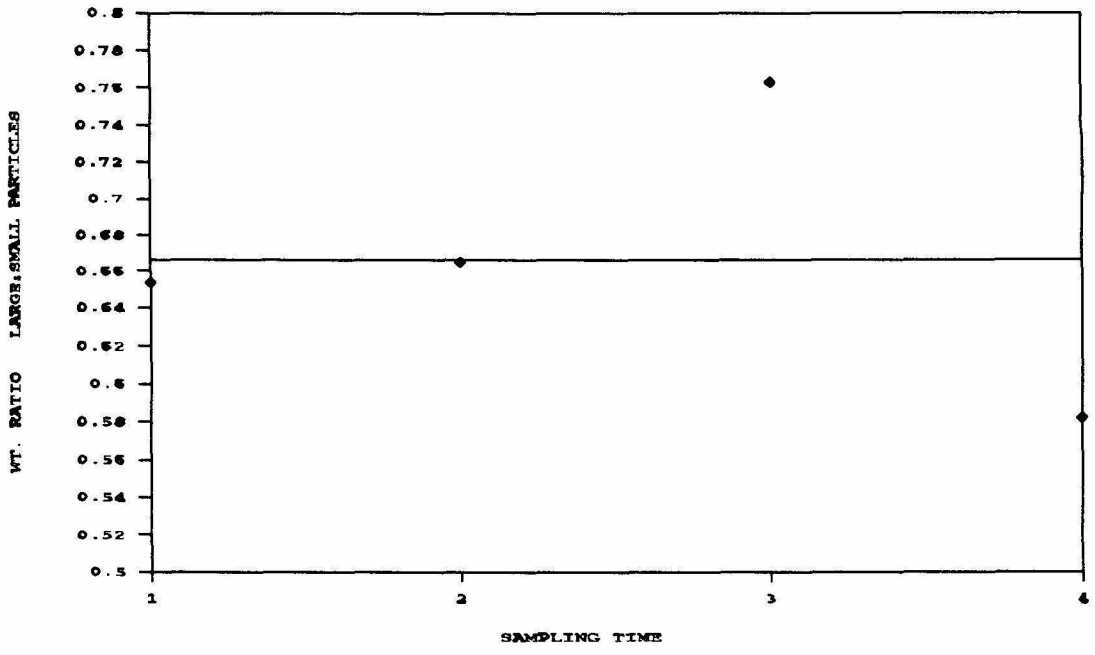

Figure 11. Variation of Mass Ratio at Channel Discharge

found that when a binary mixture of particles with a size ratio less than 3:1 is allowed to travel in conical, funnel flow through a hopper, segregation becomes significant during the final transient. Flow occurring during the earlier, steady-state, portion of the discharge, exhibits negligible or no segregation. The final transient occurs when the top surface of particles falls to a level corresponding to the top of the converging flow region in the hopper. In this portion of the flow, there is a retention of small particles in the hopper within the stagnant regions on either side of the central flow region.

This type of segregation behavior appears to be the same as that occurring during the experiments detailed in this paper. Although this hopper design is different from that used by Arteaga and Tüzün, being of a rectangular cross section rather than circular, the effect of the sloping sides results in small particle percolation downward to these sides.

Thus, for the "steady state" portion of flow, the mass ratio remains constant. The

small particle downward percolation during the "final transient" portion of the flow results in a small particle deficit at the hopper exit for the initial stage of this transient, as particles from the top surface, flow over the stagnant "corners" of the hopper. The end of the transient shows an increased concentration of small particles as shown in figure 11. As the first, steady-state, portion of a run produces a constant mixture ratio at the hopper discharge, care was taken to obtain data during this regime.

D. Image Processing

The images recorded on video tape were next captured by the image processing system. A region of 1.25 cm in length and a width appropriate to match the channel width was selected for each case. A pixel width setting of three was used to set the physical size of the pixel to a square with equal width and length. Forty pixel rows are required to span the selected 1.25 cm physical length of the selected region.

Due to storage limitations of pixel data within the image processing system, 200 buffers of data are used for each case. This allows an equal number of buffers for both channel widths to be stored and processed. To span a large portion of an individual test run, pixel data was captured at an interval of 1/10 second between buffers. This allows data over 20 seconds of a test run to be found and averaged.

Individual buffers of pixel data are low-pass filtered. Figures 12 and 13 show pixel images as recorded for a 75% small particle case (test series 7). The data shown in figure 12 is near the bottom of the channel, X/H = 40.0, figure 13, at the channel

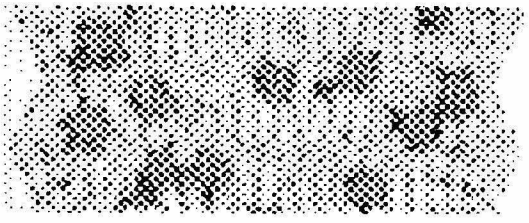

Figure 12. Image As Captured X/H = 40.0, 75% Small Particles

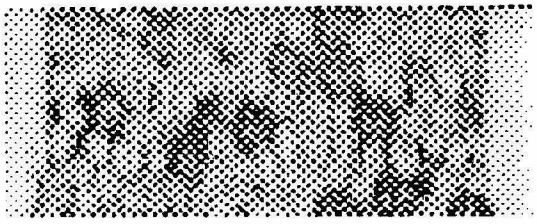

Figure 13. Image As Captured X/H = 0.0, 75% Small Particles

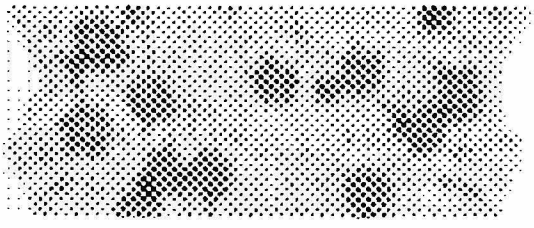

Figure 14. Image of Figure 12 - After Low-Pass Filtering

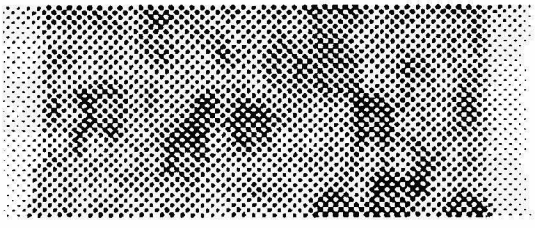

Figure 15. Image of Figure 13 - After Low-Pass Filtering

entrance. Figures 14 and 15 present this image after low-pass filtering.

The histograms for the four images (figures 12-15) shown are presented in figures 16 through 19, respectively. The histogram plots show the number of pixels in the image at each pixel value. The unfiltered data show a scattering of points without the desired double peak (figures 16 and 17). When the pixel data are low-pass filtered, peaks representing concentrations of the two colors of particles can be seen. The peak on the left side, for lower pixel values, represents the larger, darker, blue particles. The right peak represents the smaller, lighter colored, yellow particles.

Histogram data for each of the 200 buffers obtained for a test run are averaged to compensate for slight shifts in lighting values. The averaged histograms are shown in

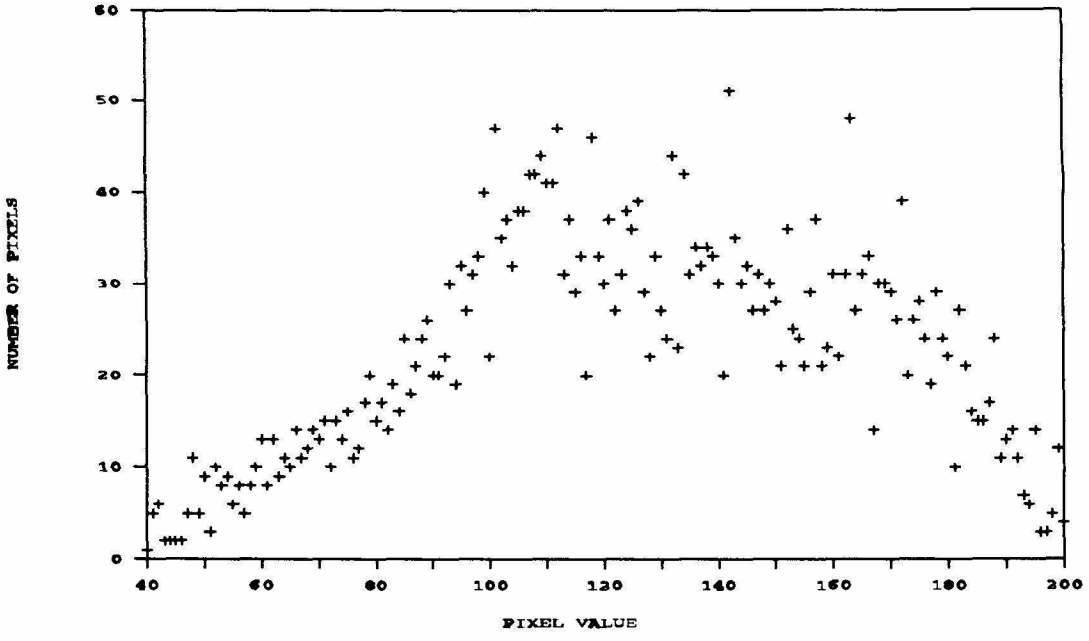

Figure 16. Histogram Data for as Captured Image seen in Figure 12

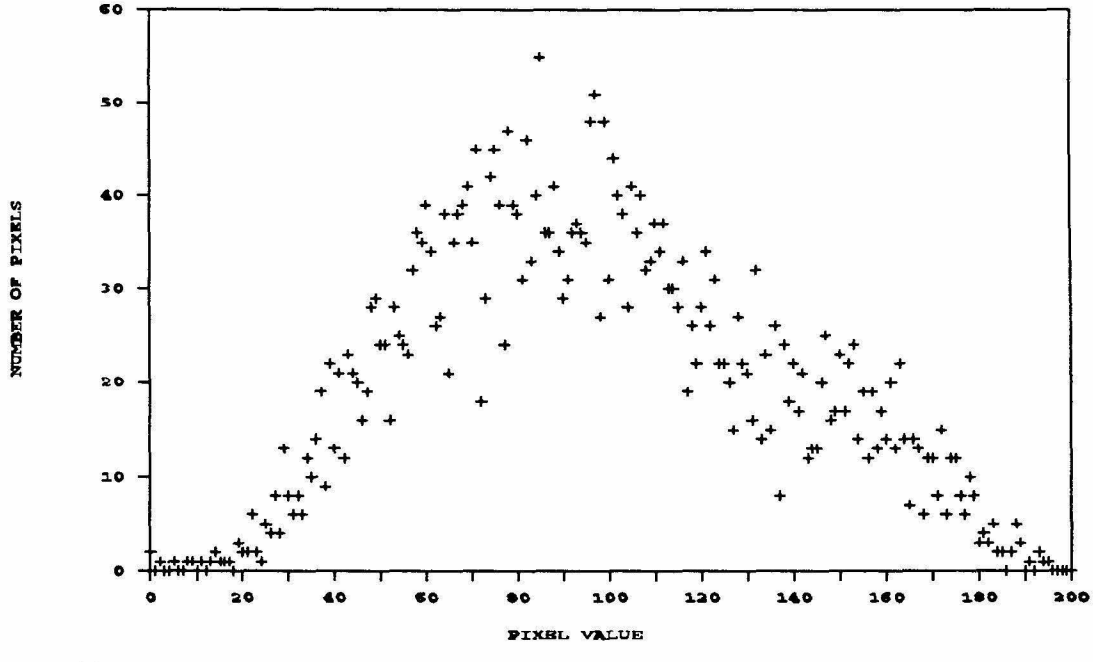

Figure 17. Histogram Data for as Captured Image of Figure 13

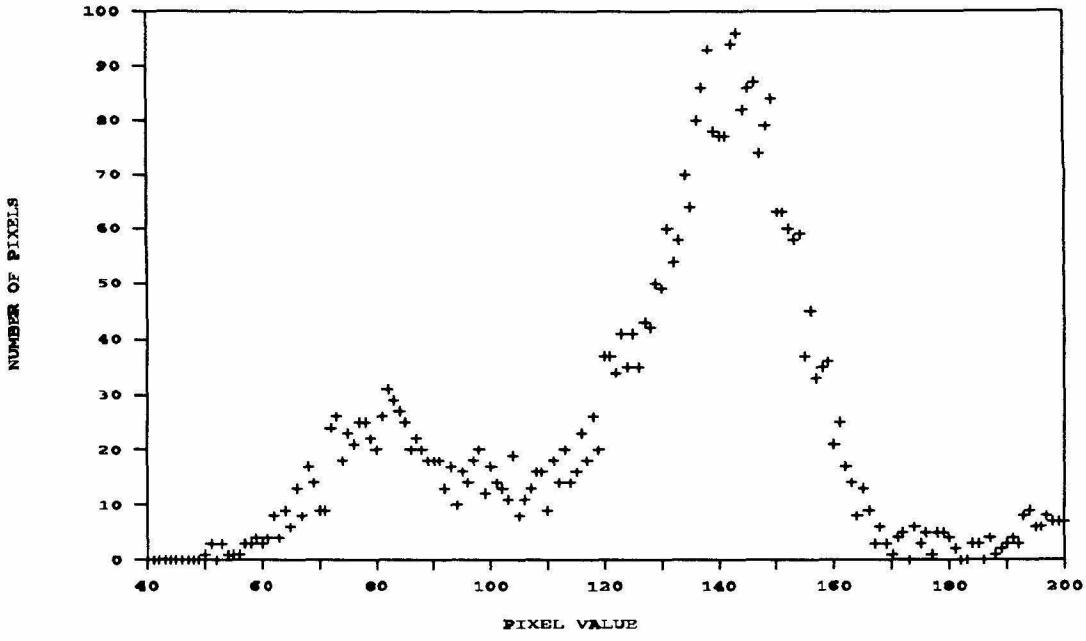

Figure 18. Histogram Data for Filtered Image of Figure 14

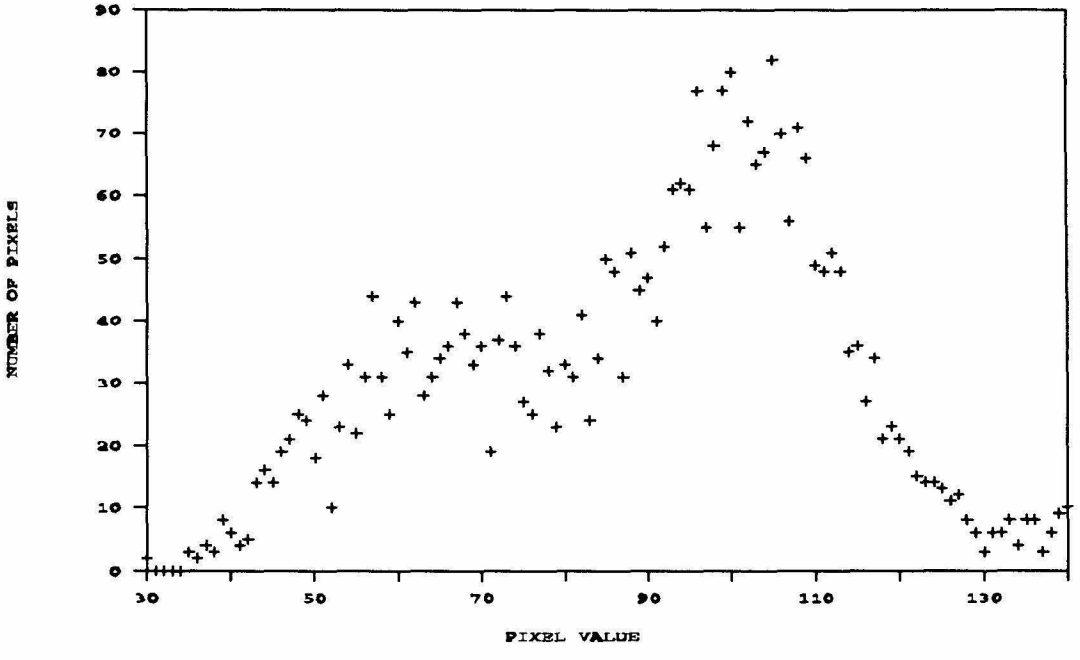

Figure 19. Histogram Data for Filtered Image of Figure 15

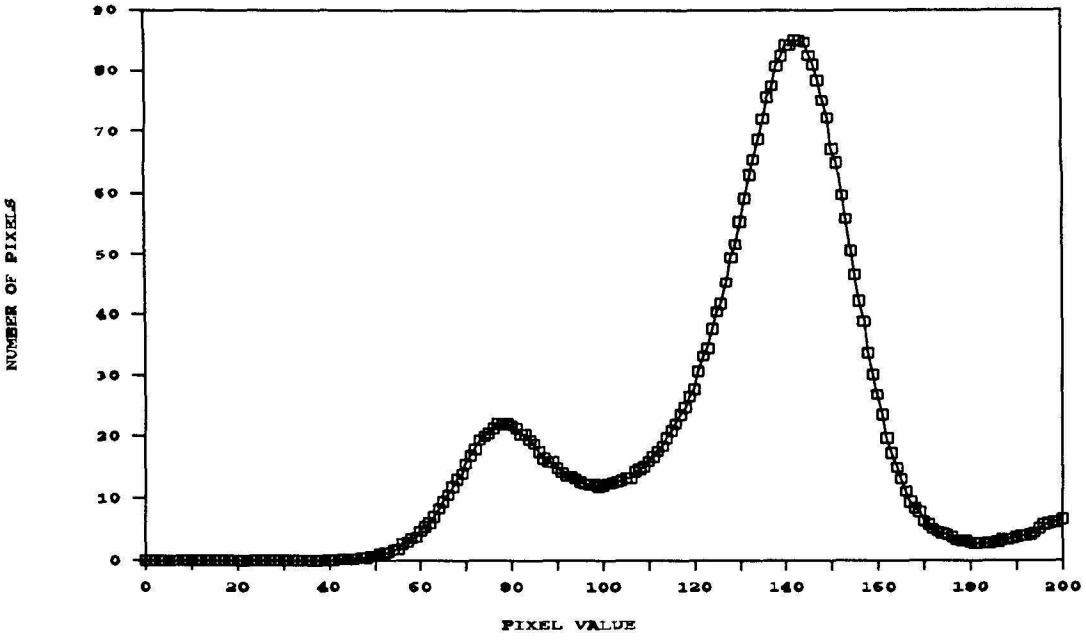

Figure 20. Averaged Histogram Data for Series of 200 Images. X/H = 40.0

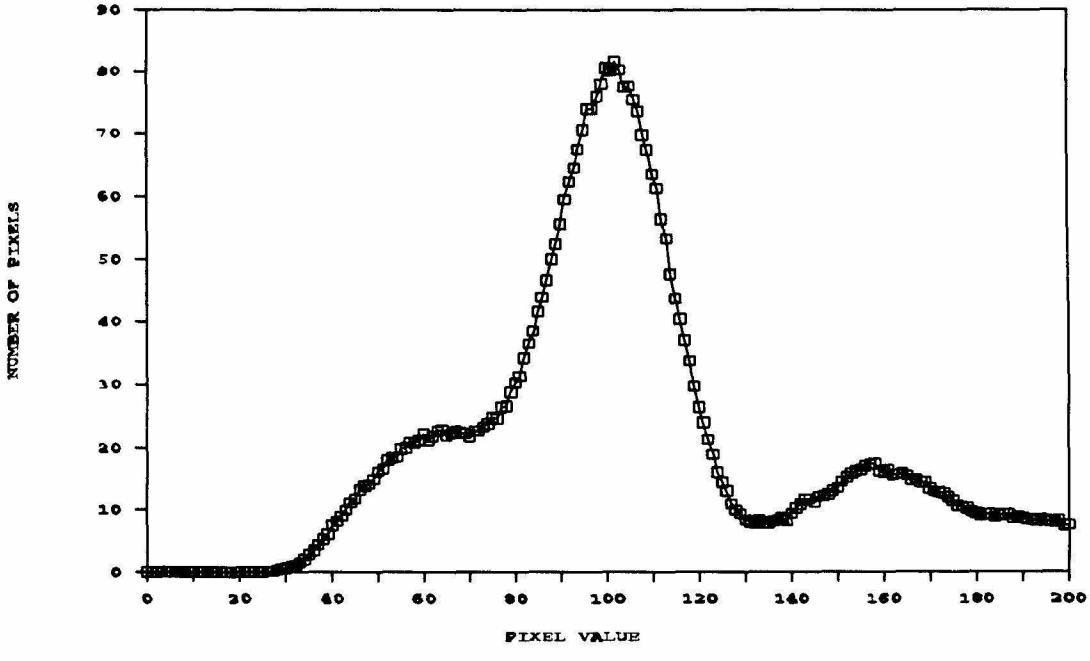

Figure 21. Averaged Histogram Data for Series of 200 Images. X/H = 0.0

figures 20 and 21. The minimum value between the two peaks is selected to divide histogram data into pixel values representing yellow particles and those representing blue. The images captured at the entrance to the channel have less light than other locations, and therefore show lower overall values on the 0 - 255 pixel grey scale. The peaks for these cases are less discernable than for the other channel positions.The selected minimum pixel value between the two peaks is used to enhance the images in each buffer. Pixel images with values less than the minimum, are set to a pixel value of 0, those greater are set to 255. After enhancement, all pixel values are either black or white, 0, black, representing the larger particles, 255, white, the smaller. Pixel images after the enhancement process are shown in figures 22 and 23.

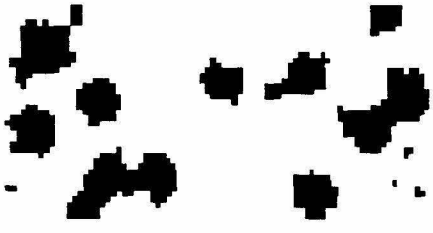

Figure 22. Enhanced Image
Original Image Shown in Figure 12

Figure 23. Enhanced Image
Original Image Shown in Figure 13

Each of the 200 buffers containing enhanced images are averaged together to obtain a time averaged pixel value at each pixel location. The resulting image represents data averaged over 20 seconds. In figures 24 and 25 the time averaged image is shown. Regions of lighter color have a greater incidence of small particles, whereas darker regions show a preferred location of larger particles. For the sawtoothed case, small

particles are present in large numbers in the areas surrounding the teeth and in vertical stripes between the channel axis and walls. During the test runs, small particles were observed to trace the tooth contour.

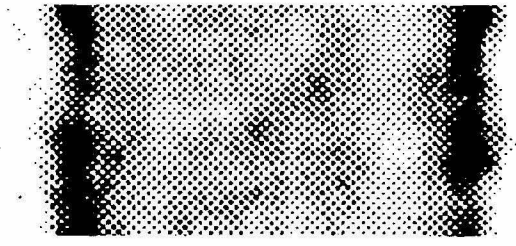

Figure 24. Image Averaged Over 20 Seconds (200 Buffers). X/H = 40.0

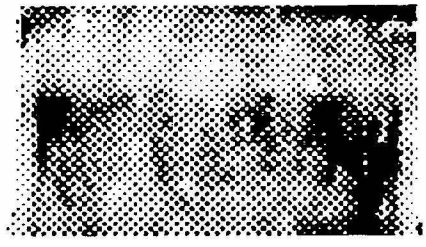

Figure 25. Image Averaged Over 20 Seconds (200 Buffers). X/H = 0.0

E. Velocity and Mass Flow Rate

The mass flow rate for each set of testing conditions was obtained by timing a known weight of particles at the channel discharge. Averaged velocity values in the channel were calculated, curves showing the influence of weight ratio and valve setting on velocities are presented in figures 26 and 27. Figure 26 shows the dependence of velocity on the exit area for the three weight ratios used. In figure 27, the effect of weight ratio on velocity for a constant exit area may be seen.

As the exit area is increased, the average channel velocity increases in linear fashion. Mixtures with larger concentrations of small particles have a higher average velocity than those with predominately larger particles. Similar results were also produced by Arteaga and Tüzün (1990).

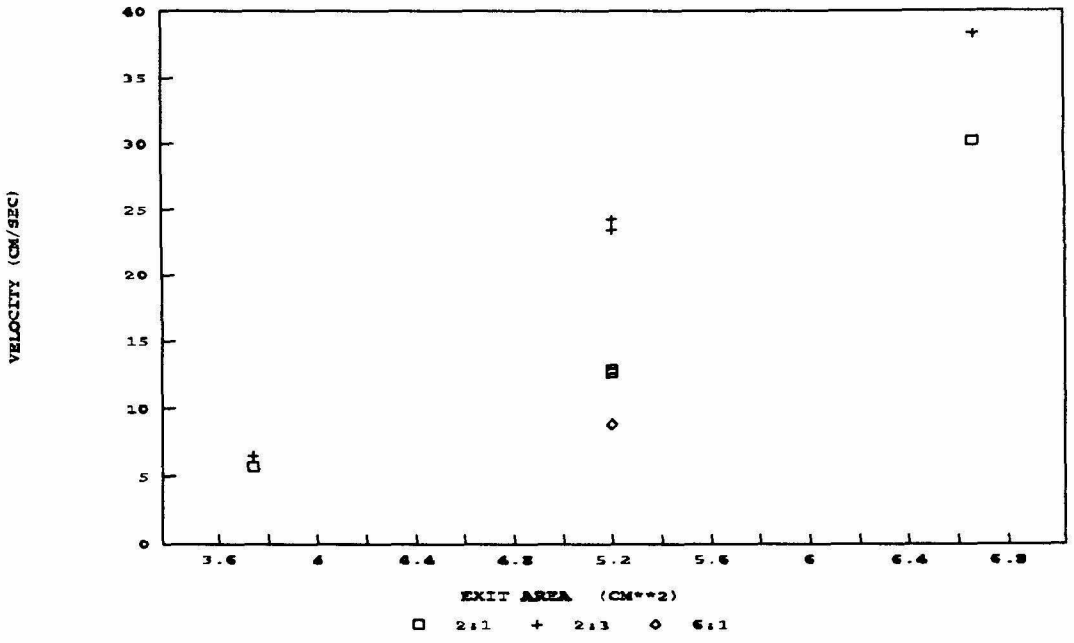

Figure 26. Velocity Dependence on Exit Area for Differing Weight Ratios

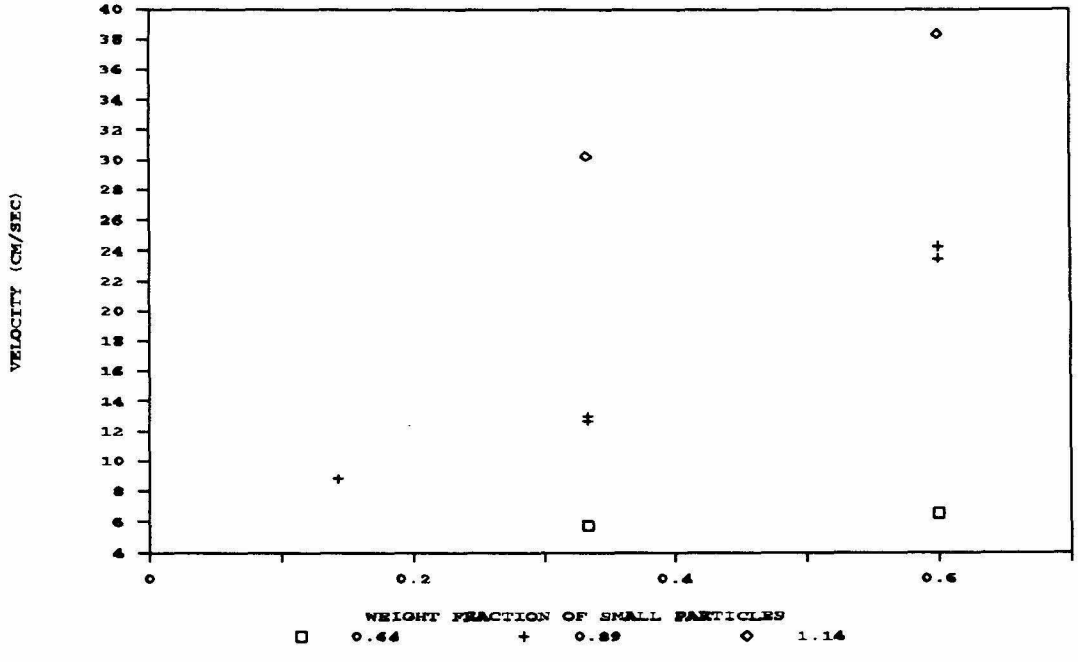

Figure 27. Velocity Dependence on Weight Ratio for Differing Exit Areas

The linearity of these results also match those obtained by Zeininger, Patton and Brennen for a similar diameter ratio.

F. Presentation of Results

At least three test runs were performed for each set of test conditions. For each run, the upper hopper was refilled with particles and flow was allowed to commence by opening the lower valve. The pixel data for each test run was processed as outlined above, after which each vertical column of data was averaged, reducing a matrix of pixel data representing concentrations at each pixel location, to a row of data representing pixel values averaged over time and a 1.4 cm length of channel. The corresponding rows were again averaged for each test run under the same test conditions, at the same location. The pixel values were normalized such that a concentration value of 0.0 represents zero small particles, all large particles, and a value of 1.0 represents all small particles. The following series of graphs present these concentration profiles across the width of the channel plotted at the four vertical locations within the channel at which data was obtained: X/H = 0.0, X/H = 13.33, X/H = 26.67, and X/H = 40.0 for the narrower channel, X/H = 0.0, X/H = 10.0, X/H = 20.0, and X/H = 30.0 for the wider channel (test series 6). The concentration values shown represent the fractional average concentration of small particles over 200 buffers.

The developing channel concentration profile may be observed for each test series. The concentration of particles at the entrance to the channel appears relatively uniform

in test series 1-4, 6-8 and 10, allowing for difficulties in lighting of this region. Concentrations of smaller particles near the walls can be seen, even at the channel entrance, but this is partially due to the hopper and variable wall design, the hopper is tapered to a 15.24 cm width. At a channel width of 3.81 cm, this design allows a horizontal surface, 5.7 cm long, along which small particles collect. Smaller particles then flow around the corner of the horizontal base of the hopper and into the channel for both types of wall conditions, producing the increase in the small particle concentration at the walls.

The glass wall concentration profiles (figures 28 and 29) appear much flatter than those of the sawtooth walls. These results were anticipated since glass channel sidewalls provide less shearing than do the sawtoothed walls. The velocity profiles for uniformly sized 3 mm particles in this channel were measured using two fiber-optic probes by Hsiau and Hunt (1992). The smooth walled channel was found to have a flat velocity profile, while the sawtooth walled channel shows steep velocity gradients at the wall. With a higher concentration of small particles, some segregation of particles is noted close to the side walls (figure 29).

The series that were run for differing ratios of particles with otherwise similar channel conditions (figures 30, 34 and 37), (3.81 cm channel width, 0.89 cm valve setting) show some differences in behavior. The concentration profiles take on different shapes. Figure 30 shows the results from a 2:1 large to small mass ratio particle mixture. Large concentrations of small particles are seen at the side walls. The larger particles have a preferred location at a position about 80% of the distance between the channel

centerline and the side walls. When the concentration of small particles is increased to a ratio of 2:3, the concentration profile contains an increased incidence of smaller particles at the centerline (figure 34). Where there had been a deficit of small particles at the centerline of the channel, the profile has become flatter. On the other hand, when the concentration of small particles is reduced to a mass ratio of 6:1, fewer small particles appear concentrated at the side walls, with the center region of the channel showing the small particles deficit as is seen for the middle value of mass ratio (figure 37).

The effects of increasing or decreasing the channel width can also be seen in the series of figures. Under faster flow rates, the top of the channel is not always filled to the sides with particles, causing the concentration value readings to be low in this region due to averaging empty channel color along with the particles (figures 32 and 36). At other locations in the channel this problem does not exist; the particles are closely packed across the width of the channel and therefore the pixel values are more accurate.

Figure 28. Test Series 1: Glass Walls, 2:1 Mass Ratio, 3.81 cm Width, 0.89 cm Valve

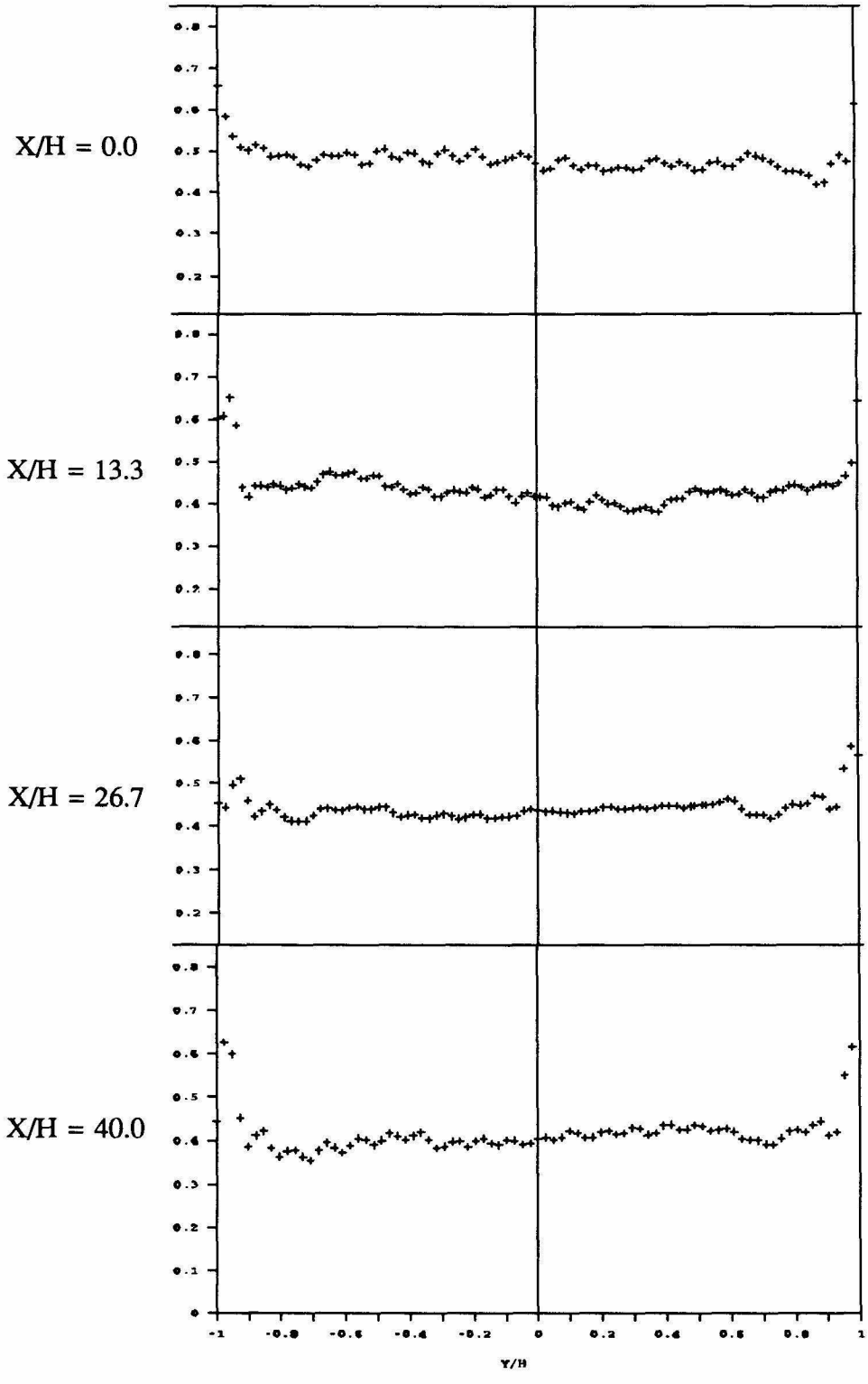

Figure 29. Test Series 2: Glass Walls, 2:3 Mass Ratio, 3.81 cm Width, 0.89 cm Valve

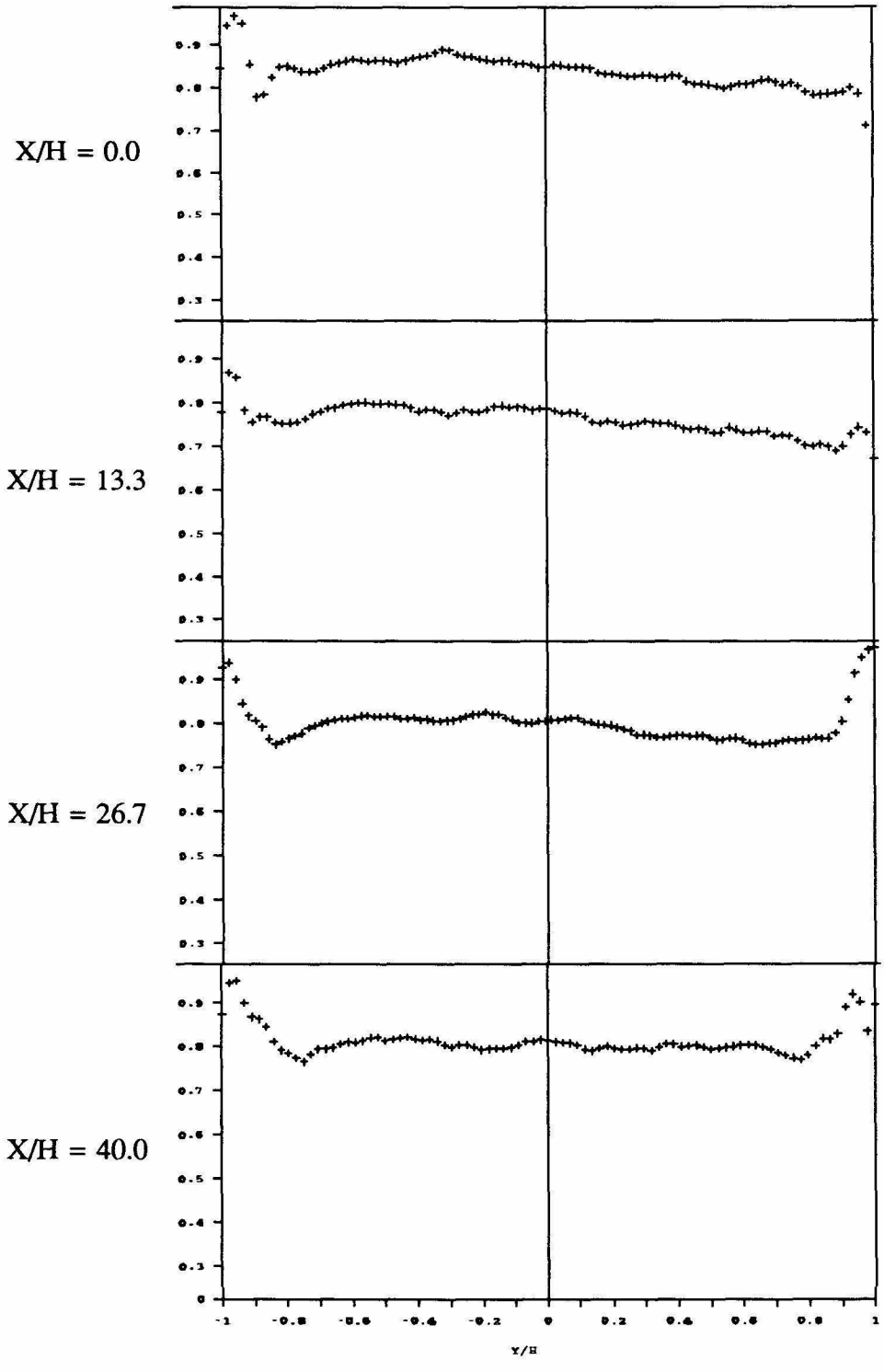

Figure 30. Test Series 3: Sawtooth Walls, 2:1 Mass Ratio, 3.81 cm Width, 0.89 Valve

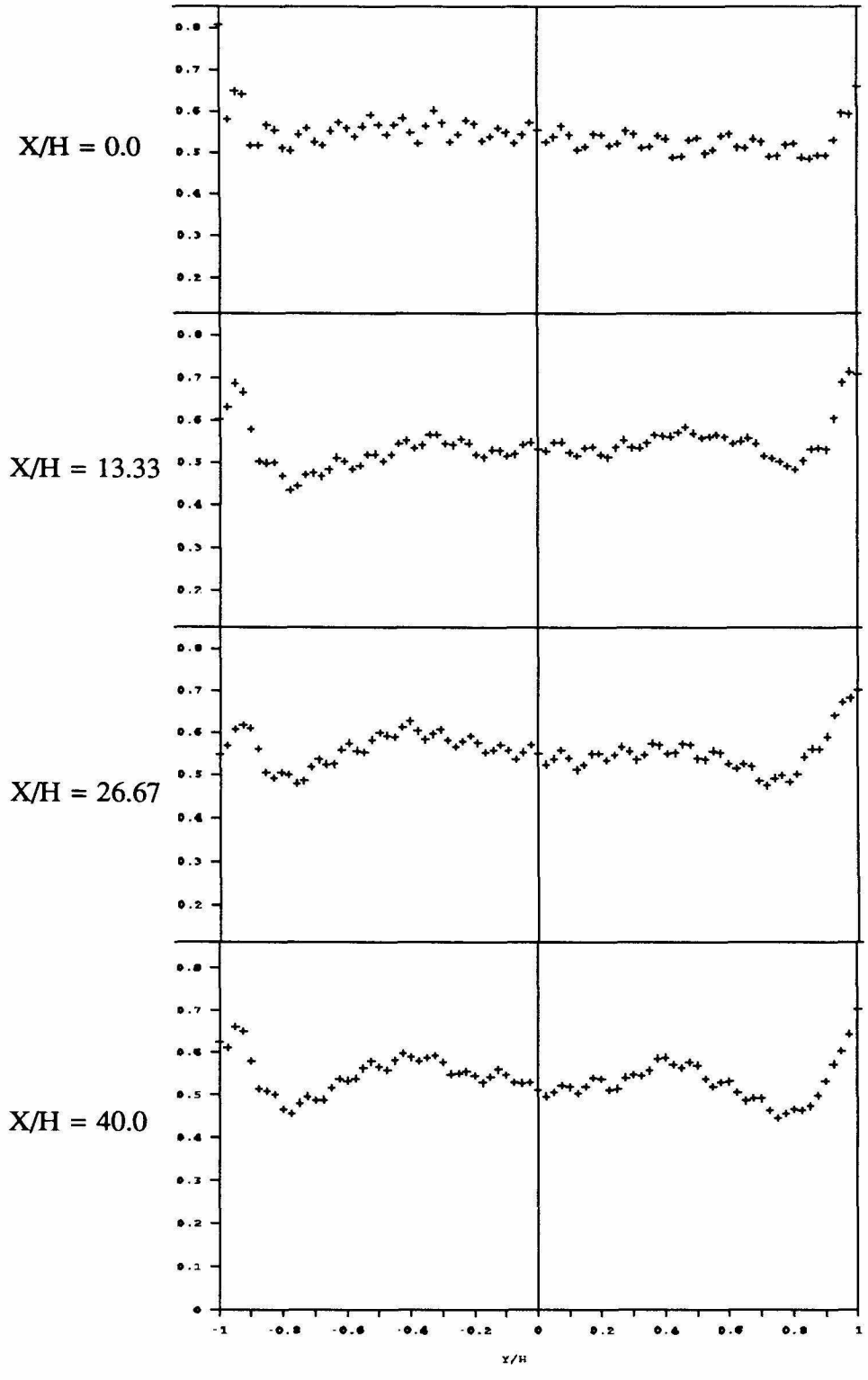

Figure 31. Test Series 4: Sawtooth Walls, 2:1 Mass Ratio, 3.81 cm Width, 0.64 Valve

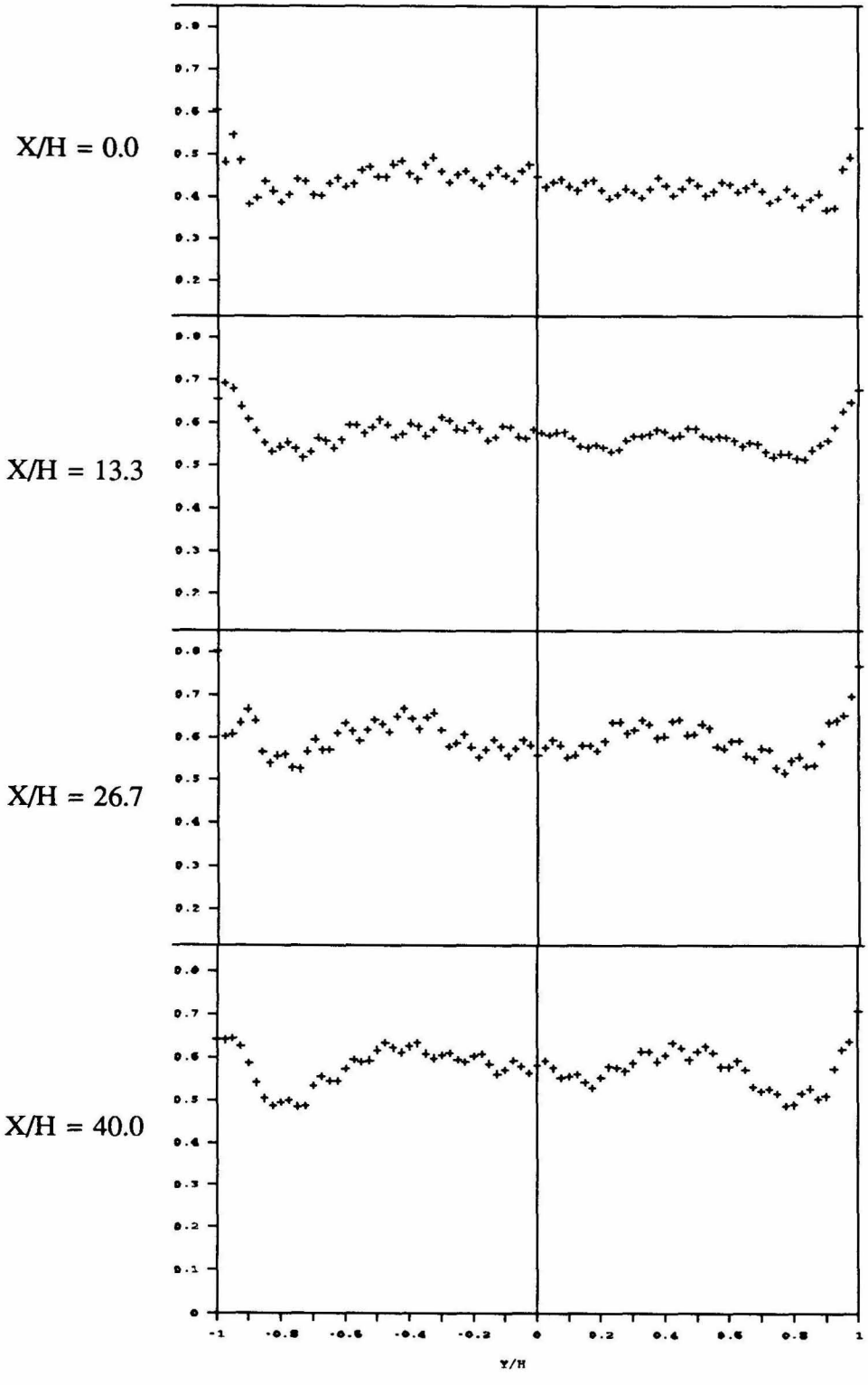

Figure 32. Test Series 5: Sawtooth Walls, 2:1 Mass Ratio, 3.81 cm Width, 1.14 Valve

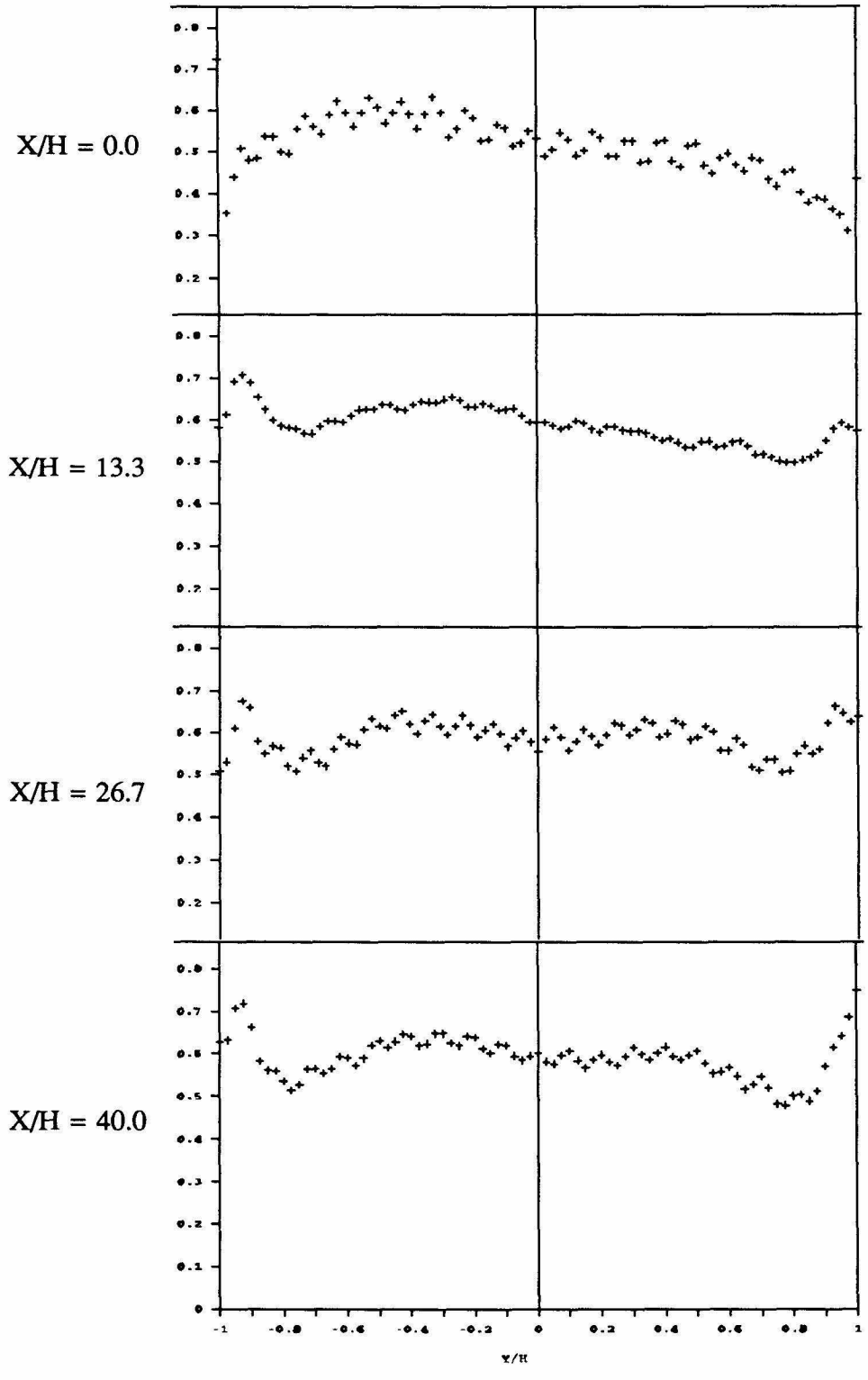

Figure 33. Test Series 6: Sawtooth Walls, 2:1 Mass Ratio, 5.08 cm Width, 0.89 Valve

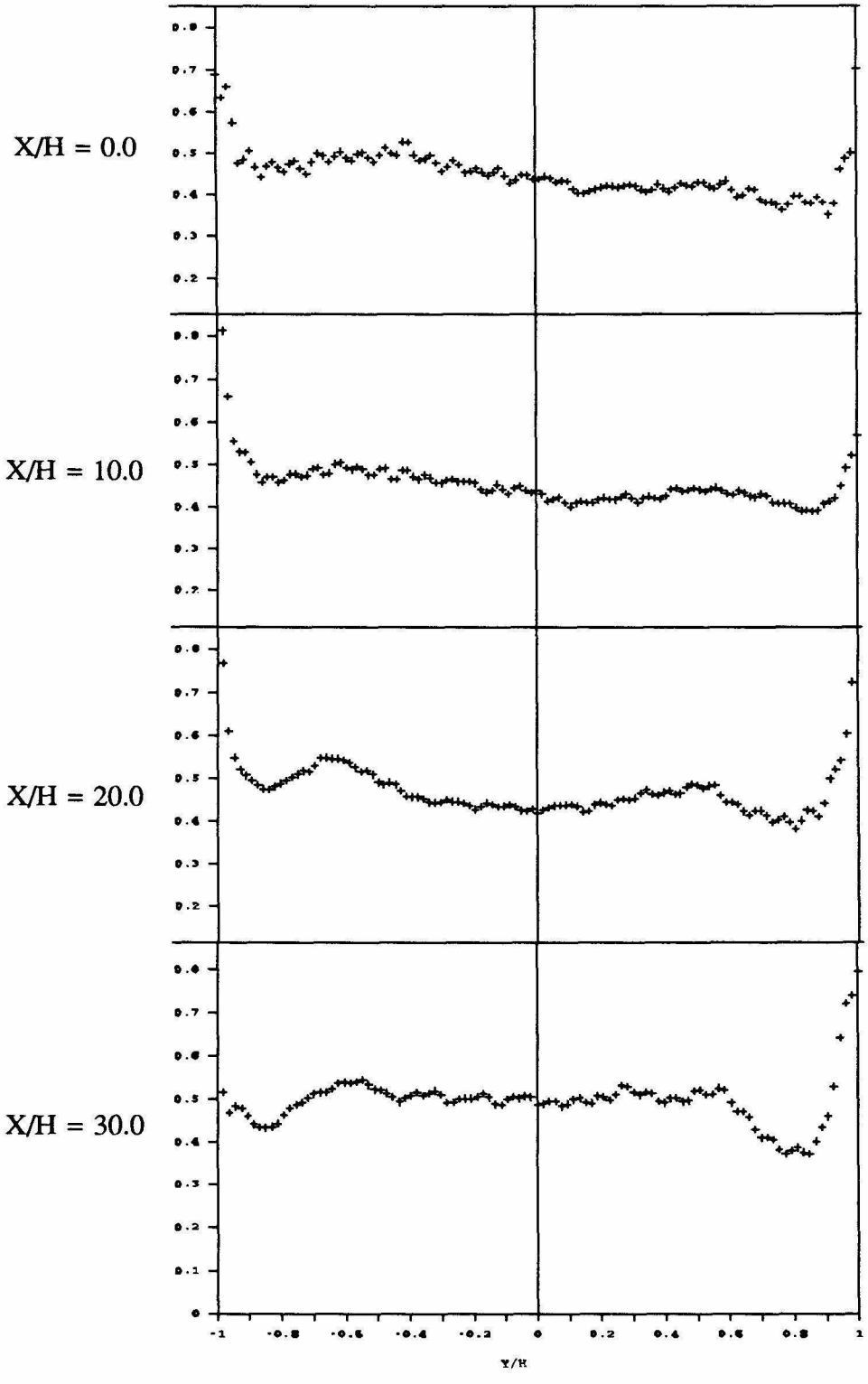

Figure 34. Test Series 7: Sawtooth Walls, 2:3 Mass Ratio, 3.81 cm Width, 0.89 Valve

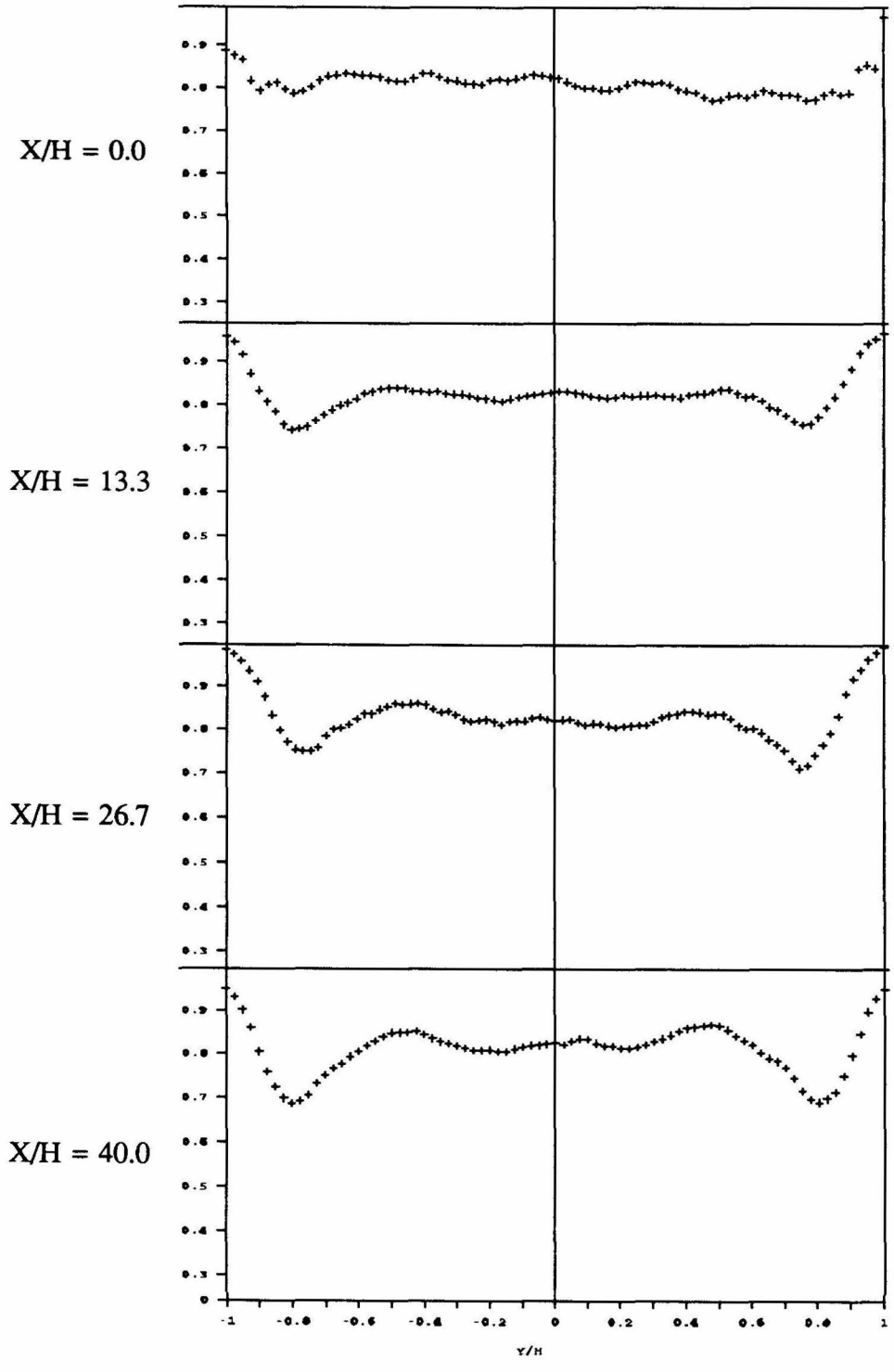

Figure 35. Test Series 8: Sawtooth Walls, 2:3 Mass Ratio, 3.81 cm Width, 0.64 Valve

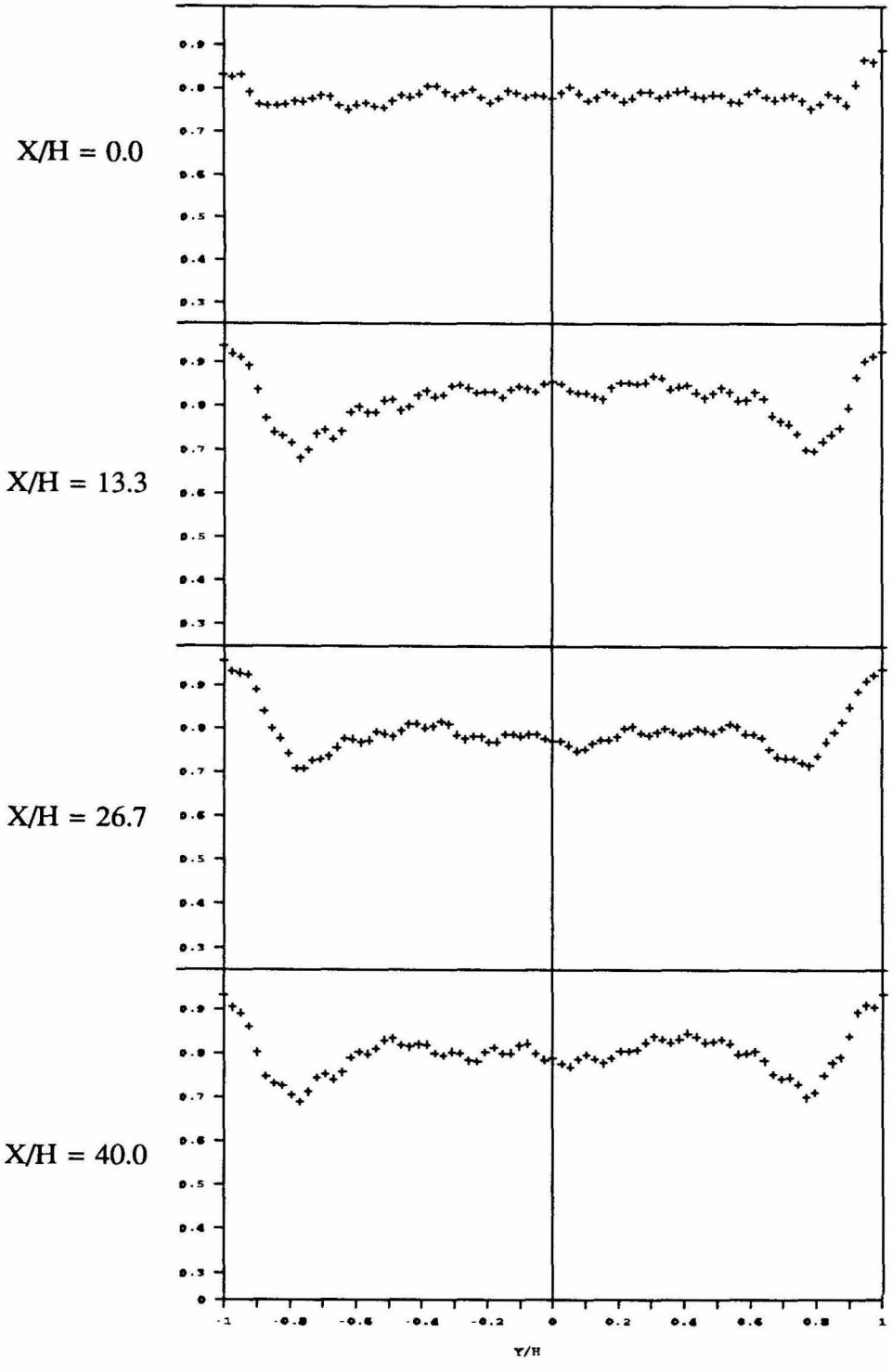

Figure 36. Test Series 9: Sawtooth Walls, 2:3 Mass Ratio, 3.81 cm Width, 1.14 Valve

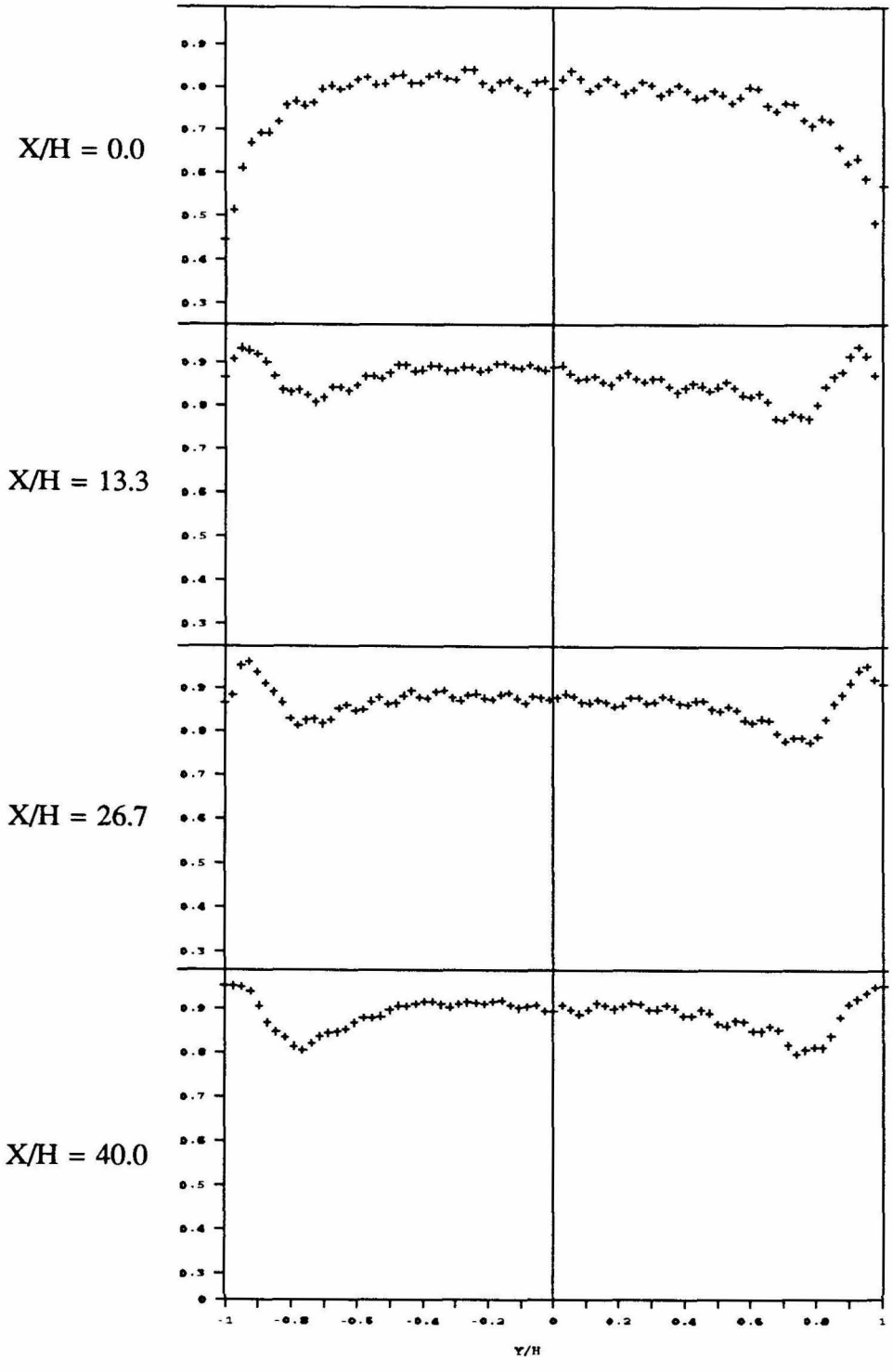

Figure 37. Test Series 10: Sawtooth Walls, 6:1 Mass Ratio, 3.81 cm Width, 0.89 Valve

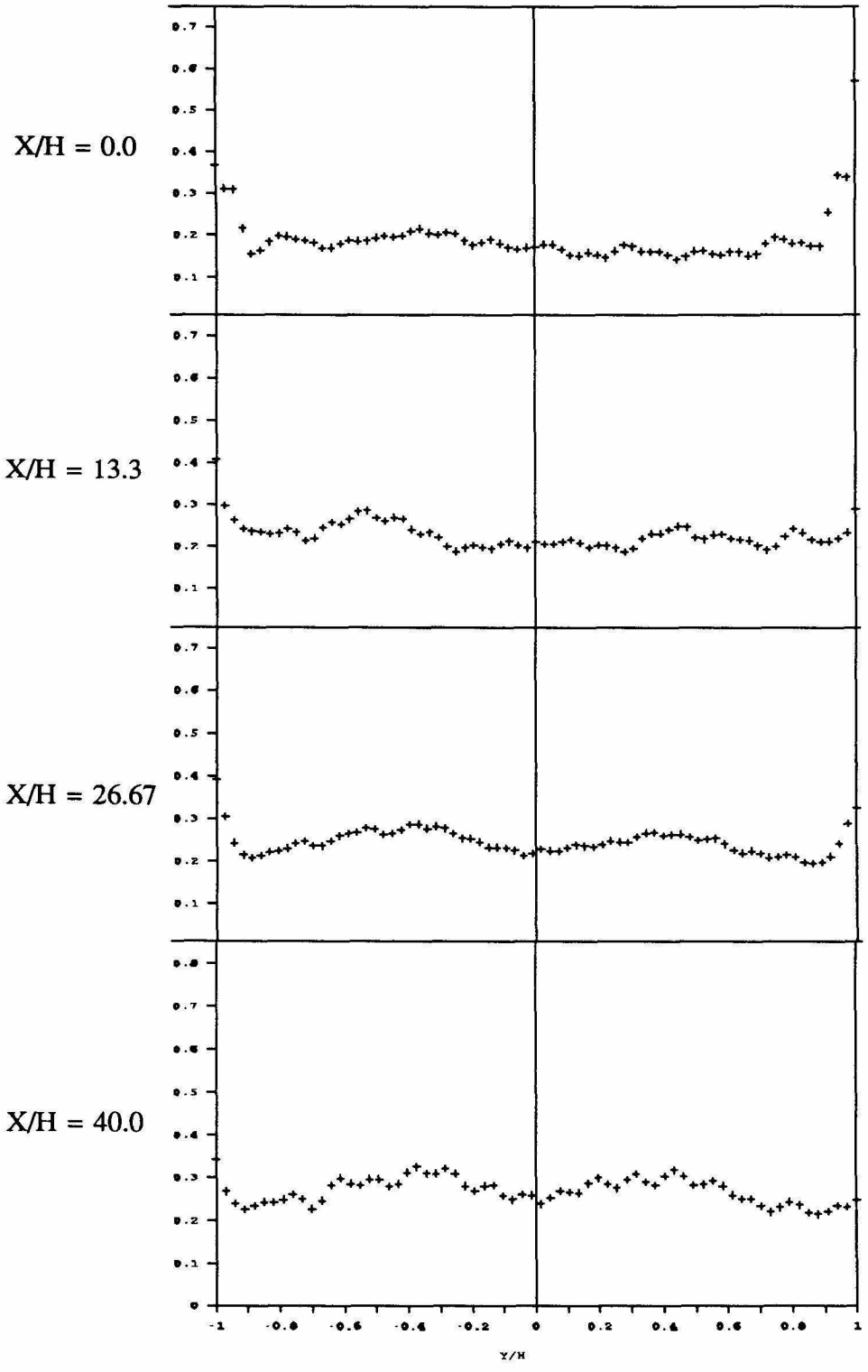

In order to compare more easily the various concentration profiles as they are developing, figures 38 - 40 are presented. Each of these figures shows the concentration difference between the minimum concentration of small particles, occurring at approximately 80% of the distance from the centerline to the sidewalls, and the maximum concentration of small particles away from the side walls which occurs at around 50% of the channel half width. This concentration deficit of small particles is shown as a function of downstream channel distance. Figure 38 compares the concentration deficit for differing mass ratios using the same valve setting. Figures 39 and 40 compare the effect of flow rate change using the same mass ratio of particles.

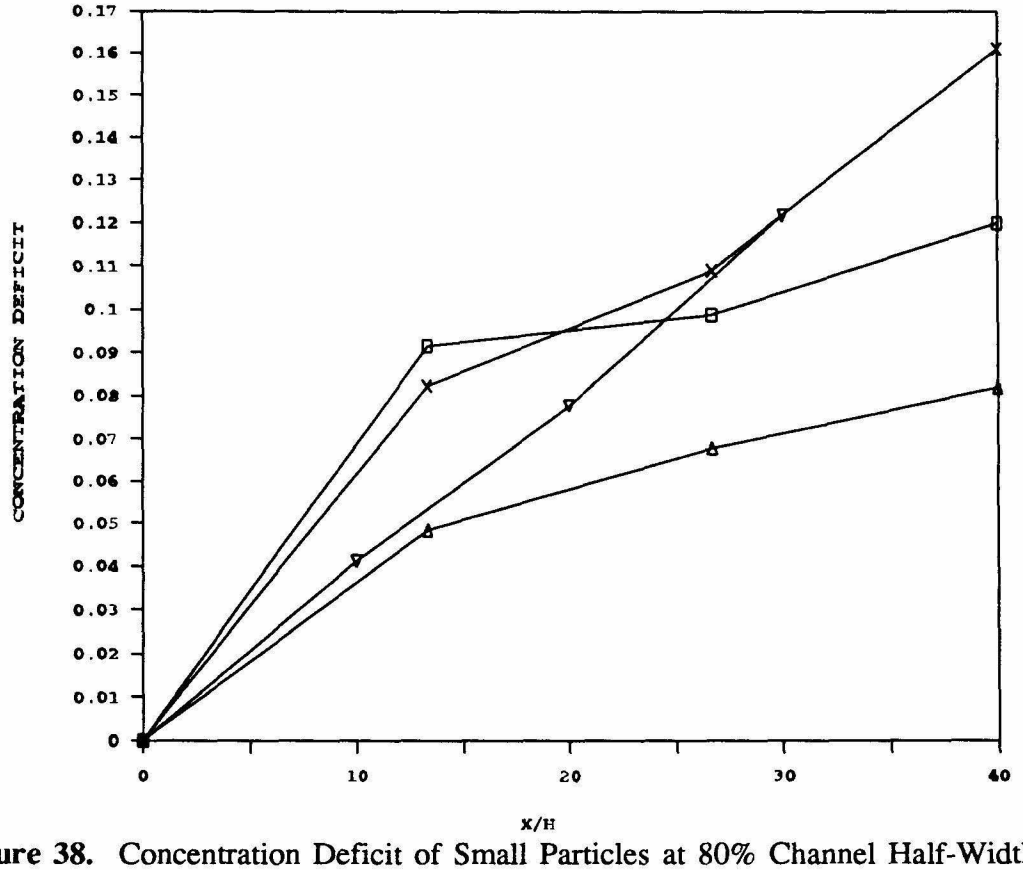

Figure 38. Concentration Deficit of Small Particles at 80% Channel Half-Width Test Series 3 (□,wt.ratio 2:1), 6 (▽,2:1,wide), 7 (x,2:3), 10 (△,6:1): Valve Setting = 0.89 cm for all Cases

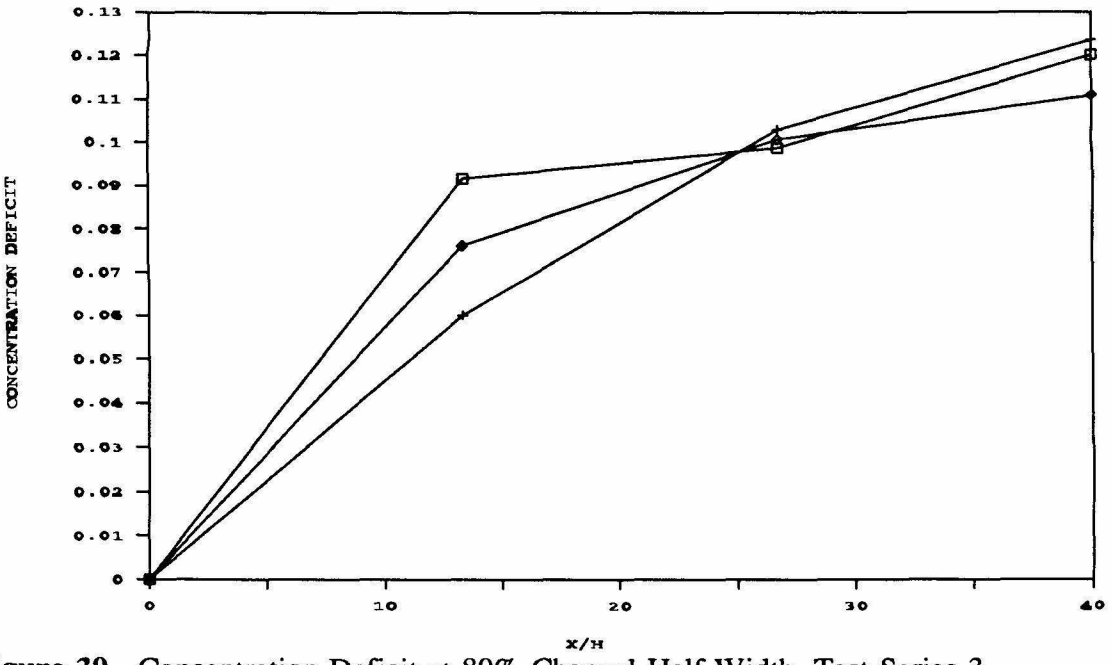

Figure 39. Concentration Deficit at 80% Channel Half-Width, Test Series 3 (□, Valve 0.89), 4 (+, Valve 0.64), 5 (◊, Valve 1.14), Mass Ratio 2:1

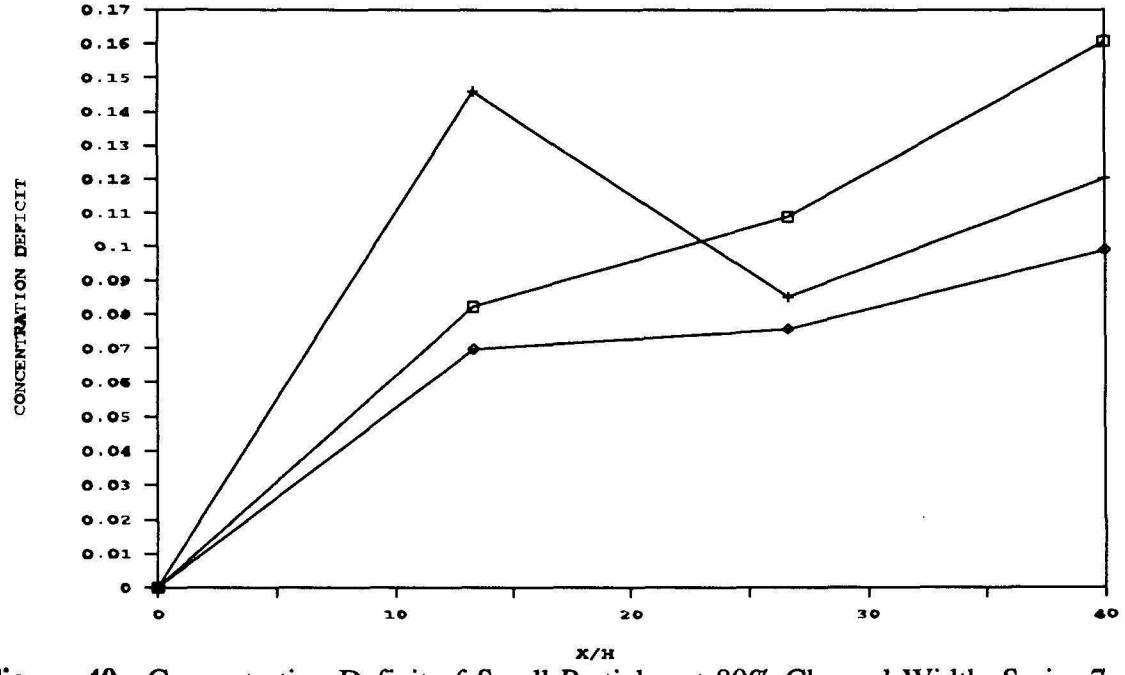

Figure 40. Concentration Deficit of Small Particles at 80% Channel Width, Series 7 (□, Valve 0.89), 8 (+, Valve = 0.64), 9 (◊, Valve = 1.14), Mass Ratio 2:3

The data presented in the concentration deficit series is obtained after using a smoothing function on the data presented in the previous set of curves (figures 31 - 37). The deficit value represents the average of the deficits found on either side of the centerline.

The glass side wall profiles indicate minimal segregation. The small particle concentrations along the side walls at the channel entrance appear to be due to entrance conditions caused by segregation in the upper hopper. Profiles do not exhibit large variations at the side walls for varying channel locations.

As glass front and back walls were used in the channel, it is interesting to note third-dimensional effects occurring through the depth of the channel, caused by segregation along these surfaces. An indication of the amount of segregation across the

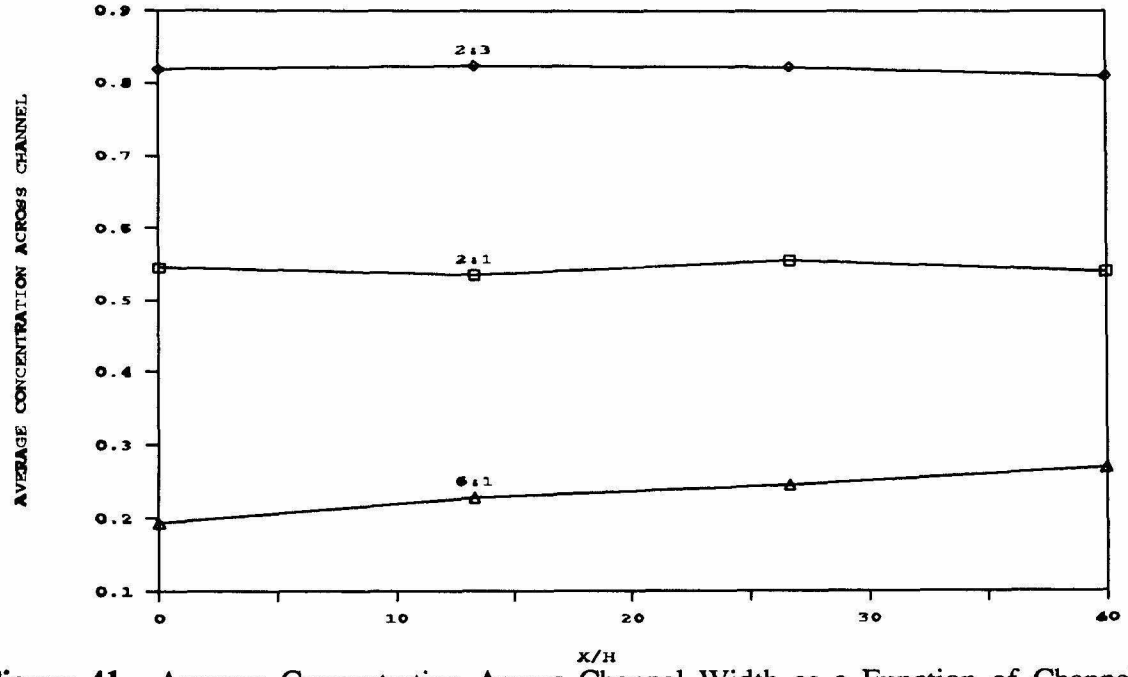

Figure 41. Average Concentration Across Channel Width as a Function of Channel Position (X/H) for Varying Weight Ratios - Sawtoothed Walls

depth would be the averaged concentration value over the channel width at varying X/H positions. If smaller particles were moving toward or away from the glass walls, the averaged concentration values at each location would vary. The averaged concentration values as a function of X/H position are observed in figure 41. Minimal changes are noted for the 2:1 and 2:3 weight ratio cases. The 6:1 case indicates some overall concentration changes along the length of the channel. This indicates some segregation across the channel depth when large numbers of larger particles are present.

III. DISCUSSION

A series of experiments was run to enable calculation of concentration profiles as a function of channel width at various locations in a vertical channel. Image processing techniques were used to obtain color values averaged over time within the channel. The time averaged color value at a location within the channel is a measure of the average concentration at that location. Color values were normalized so that direct particle concentration values within the channel were obtained. A value of 0.0 for concentration represents 100% large particles, 1.0, 100% small particles. The resulting fractions therefore, indicate the fraction of time a small particle occupies that position.

The test conditions were varied to note the effect on particle concentration profiles. Parameters varied include: mass ratio of large to small particles, side wall surface conditions, channel width, and mass flow rate. Concentration profiles are presented in figures 28 - 37. Values of concentration are shown as a function of channel width at four locations within the channel. Development of concentration profiles can be seen in this series of figures.

Glass side walls provide concentration profiles that are relatively flat compared to those produced using the sawtoothed walls. With a particle mass ratio of 2:3, more variation of concentration across the channel is noted than for the 2:1 case. The flow within the channel for all glass wall runs was not totally smooth. Surging was noted in some cases, it is unclear what effect these fluctuations may have on the concentration

profiles developed.

When the walls were changed to sawtoothed, distinctive profiles develop within the channel for all three particle mass ratios. When a 2:1 mass ratio is used, the effect of mass flow rate changes appears to be minimal. The profiles are virtually identical for the three valve settings that were used. The larger particles tend to migrate to a position at approximately 80% of the channel width from the centerline, small particles have peak concentrations at the side walls and at around 50% channel width. At the centerline of the channel a decrease in concentration of small particles is also noted; however the magnitude of this deficit is about half that seen at the 80% position. As the flow rate is increased, the profile of the centerline region flattens.

As the channel width is increased, while fixing the mass ratio and valve settings, the developing profiles appear identical to those of the narrower channel at the same X/H (channel width/distance vertically downward along the channel) position.

Changing the mass ratio of the particle mixture to a mix containing an increased number of smaller particles (from a mass ratio of 2:1 to 2:3), resulted in profiles which were very similar to the previous set. Concentration values again indicate a higher number of larger particles at the 80% position. Profiles in the centerline region also show an increased number of large particles, but the profiles appear flatter for this increase in small particles. The profiles for the fastest flow rate case are much flatter overall than any of the earlier cases. The concentration deficit values are also not as large at the 80% location.

Decreasing the concentration of small particles to a mass ratio of 6:1 changes the

concentration profiles more dramatically. The preferred position of large particles is shifted closer to the channel walls, to a position of 90% of the channel centerline to wall distance, instead of the 80% position seen in the previous mass ratios (figure 37). The curves appear flatter overall, with a decreased value of concentration deficit relative to those seen in any of the previous sawtoothed cases. The centerline of the channel does show a concentration deficit of small particles, but the peak concentration of small particles on either side of the centerline has moved to a position of 40% of the channel half-width from the 50% of previous cases.

Figures 38 - 40 illustrate the magnitude of the difference in concentration of small particles at the 80% position preferred by the larger particles relative to the peak concentration of small particles occurring at the 40% - 50% channel half-width position. This concentration deficit is shown as a function of normalized vertical channel distance traversed by the particles. In general, the concentration deficit increases with distance. The channel was not long enough to note if any "steady state" concentration profiles develop.

Concentration values across the channel width are averaged at four vertical channel positions and are presented in figure 41 for each of the mass ratios used. The curves appear flat for the 2:3 and 2:1 mass ratios, a small increase in overall concentration of smaller particles with distance is observed in the 6:1 case, demonstrating that for a greater relative number of larger particles, some segregation in the vertical direction is also seen. This segregation is most likely due to gravity as some of the smaller particles percolate downward resulting in increased numbers of smaller particles at the lower levels.

IV. CONCLUDING REMARKS

Work by previous researchers has shown that particle segregation by size exists when a granular material is in motion. Many of these studies involved determining the amount of segregation, which was due in part to gravitational effects, by capturing the particles, sorting by size, and measuring the relative quantities.

This study was undertaken to determine if particles segregate by size in the direction transverse to the gravitational field due to effects of wall shearing. In an effort to determine concentration profiles over the length and width of the channel without disturbing the flow, measurement was made by employing image processing techniques to obtain a time averaged view of the flow stream through the glass front wall of the test channel.

The image processing methods used proved quite satisfactory in determining concentrations. The concentration of localized areas within the channel were found by averaging color over time and space. Care was required in providing uniform coloration of particles, a sufficient color contrast between large and small particles, and, most significantly, uniform lighting to provide consistent color value for each particle size at all locations in the channel as captured by a video camera.

This experiment has successfully shown that particle segregation by size does occur, in the direction transverse to the gravitational field, when side walls producing an increased amount of shear are used. A preferential location within the channel is sought

by particles according to their size. Larger particles migrate toward a position of 80% the half-width of the channel when mass ratios of large to small particles of 2:1 and 2:3 were used. When a ratio of 6:1 was used, the larger particles sought a position closer to the side walls at 90% of the channel half-width. Segregation of particles increases as the material moved downwards through the channel, producing a deficit of small particles which continued to grow with distance. At a position of X/H = 40.0 within the channel, concentration deficits reached 0.15. This phenomenon appears over a wide range of both flow rates and mass ratios.

REFERENCES

Arteaga, P. and Tüzün, U., 1990. Flow of Binary Mixtures of Equal Density Granules in Hoppers - Size Segregation, Flowing Density and Discharge Rates, Chemical Engineering Science, **45**, 205-223

Campbell, A.P. and Bridgwater, J., 1973. The Mixing of Dry Solids by Percolation. Trans. Instn. Chemical Engrs., **51**, 72 - 74

Donald, M.B. and Roseman, B., 1962. Br. Chem. Eng., **7**,749

Hsiau, S.S. and Hunt, M.L., 1992, Shear-Induced Particle Diffusion and Longitudinal Velocity Fluctuations in a Granular-Flow Mixing Layer, Submitted To Journal of Fluid Mechanics

Foo, W.S. and Bridgwater, J., 1983. Particle Migration, Powder Technology, **36**, 271-273

McTigue, D.F., Givler, R.C., and Nunziato, J.W., 1986. Rheological Effects of Nonuniform Particle Distributions in Dilute Suspensions, Journal of Rheology, **30(5)**, 1053-1076

Savage, S.B. and Lun, C.K.K., 1988. Particle Size Segregation in Inclined Chute Flow of Dry Cohesionless Granular Solids, Journal of Fluid Mechanics, **189**, 311-335

Segré, G. and Silberberg, A., 1962. Behaviour of Macroscopic Rigid Spheres in Poiseuille Flow, Journal of Fluid Mechanics, **14**, 136-157

Williams, J.C., 1976. The Segregation of Particulate Materials, A Review. Powder Technology, **15**, 245-251

Williams, J.C. and Shields, G., 1967. The Segregation of Granules in a Vibrated Bed, Powder Technology, **1**, 134-142

Zeininger, G., Patton, S., Brennen, C.E., Granular material flows in hoppers and chutes; experiments on interstitial fluid, charge separation and mixture effects, Report No. E200.10, Division of Engineering and Applied Science, California Institute of Technology